Neuron

Article

Activity-dependent recruitment of inhibition and excitation in the awake mammalian cortex during electrical stimulation

Highlights

- High-frequency stimulation recruits inhibitory/excitatory neurons at similar rates
- Increasing stimulation amplitude more densely recruits excitatory neurons
- Increasing stimulation amplitude recruits a larger volume of inhibitory neurons
- High levels of ongoing activity diminish or suppress excitatory neuron responses

Authors

Maria C. Dadarlat, Yujiao Jennifer Sun, Michael P. Stryker

Correspondence

mdadarla@purdue.edu

In brief

How does cortical electrical stimulation affect different types of neurons in awake animals? The authors show that increasing stimulation amplitude recruits a distributed population of excitatory neurons but recruits inhibitory neurons closer to the electrode. Furthermore, evoked responses in excitatory neurons are strongly influenced by their pre-stimulus activity level.

Dadarlat et al., 2024, Neuron *112*, 821–834
March 6, 2024
https://doi.org/10.1016/j.neuron.2023.11.022

CellPress

Neuron

CellPress

Article

Activity-dependent recruitment of inhibition and excitation in the awake mammalian cortex during electrical stimulation

Maria C. Dadarlat,[1,2,4,5,*] Yujiao Jennifer Sun,[1,3,4] and Michael P. Stryker[1]
[1]Department of Physiology, University of California, San Francisco, San Francisco, CA 94158, USA
[2]Weldon School of Biomedical Engineering, Purdue University, West Lafayette, IN 47906, USA
[3]Institute of Ophthalmology, University College London, London EC1V 9EL, UK
[4]These authors contributed equally
[5]Lead contact
*Correspondence: mdadarla@purdue.edu
https://doi.org/10.1016/j.neuron.2023.11.022

SUMMARY

Electrical stimulation is an effective tool for mapping and altering brain connectivity, with applications ranging from treating pharmacology-resistant neurological disorders to providing sensory feedback for neural prostheses. Paramount to the success of these applications is the ability to manipulate electrical currents to precisely control evoked neural activity patterns. However, little is known about stimulation-evoked responses in inhibitory neurons nor how stimulation-evoked activity patterns depend on ongoing neural activity. In this study, we used 2-photon imaging and cell-type specific labeling to measure single-cell responses of excitatory and inhibitory neurons to electrical stimuli in the visual cortex of awake mice. Our data revealed strong interactions between electrical stimulation and pre-stimulus activity of single neurons in awake animals and distinct recruitment and response patterns for excitatory and inhibitory neurons. This work demonstrates the importance of cell-type-specific labeling of neurons in future studies.

INTRODUCTION

Electrical stimulation has long been used to map brain function by establishing causal links between neural activity, cognition, and behavior.[1–3] Recent technological advances have additionally positioned electrical stimulation as a clinically viable tool to treat neurological injury, disease, and disorders as well as to enable artificial sensation for neural prostheses.[4–6] These applications share a common goal: the precise control over and manipulation of neural activity patterns within and across brain regions, targeting networks of excitatory and inhibitory neurons.

The basic unit of electrical stimulation is a biphasic pulse of current, often delivered in a train of pulses that can vary in amplitude, timing, frequency, and duration. The anatomical region targeted and the choice of stimulation parameters determine the effects of stimulation on a local population of neurons and the resulting induced sensory percepts.[7–16] Electrical stimulation modulates neural activity by passing small electrical currents through an electrode, exciting neurons by depolarizing neural processes (primarily axons) that pass within a small radius surrounding the electrode tip.[17–20] These directly activated neurons, in turn, excite a secondary population of neurons that composes a significant fraction of neurons that respond to stimulation.[18,21,22] Thus, stimulation activates local networks of excitatory and inhibitory neurons. In consequence, even activation of single neurons can be consciously detected by animals.[23]

Pharmacological manipulations during neural stimulation and recording have clarified some of the circuit dynamics responsible for producing stimulation-evoked responses. The prototypical time-varying response of a single neuron to stimulation is a brief burst of excitation followed by a longer period of suppression.[24,25] Blocking transsynaptic activation of inhibitory neurons reduces stimulation-evoked suppression,[21,26] whereas blocking transsynaptic activation of both inhibitory and excitatory neurons reduces the response strength of neurons to stimulation.[21] Furthermore, reducing electrical coupling between inhibitory neurons prolongs and weakens inhibition, extending the spatial spread of neural activation.[26] Therefore, inhibitory networks shape both the amplitude and spatiotemporal properties of neural responses to stimulation; however, responses of inhibitory neurons have yet to be directly recorded during electrical stimulation.

Functional activity within circuits at the time of stimulation modulates evoked activity patterns. The influence of functional activity can be seen at the level of behavior, where motor activity, shifts in attention, and expectation of reward all alter stimulation-evoked neural responses.[27–31] This relationship becomes clearer when examined at a local neural level, where responses to single pulses are correlated with local field potential and

spontaneous activity.[32–34] Despite the profound modulation of sensory-evoked neural responses by neural activity related to behavior, the majority of previous studies were conducted in anesthetized animals or failed to account for behavior during analysis of stimulation-evoked activity patterns.[12,13,24,35,36] Characterizing the effects of ongoing neural activity on stimulation-evoked activity patterns is important for understanding how stimulation is integrated into neural circuits in awake states and affects perception and ultimately behavior.

Neural responses to stimulation become complex when stimulation pulses are delivered at high frequency, where the current delivered by a stimulation pulse interacts with activity patterns initiated by prior pulses, leading to variable temporal responses.[24,37] In general, although low stimulation frequencies are generally thought to be excitatory and correlate with the amplitude and spatial extent of neural responses,[15,38] high stimulation frequencies are often suppressive, promoting release of inhibitory neurotransmitters,[39] leading to neurons failing to respond through the duration of longer stimulation trains.[13,15] The use of dynamic, rather than fixed, stimulation amplitude and frequency over the course of stimulation helps maintain neural activity during longer stimulation trains.[16] Such indirect analysis of inhibitory neuron activity emphasizes the importance of characterizing the contribution of inhibitory neurons to network processing of electrical stimulation. These studies must be conducted in awake animals because anesthesia changes activity patterns in neural networks, including increasing synchrony between cortical layers, changing the strength and duration of sensory-evoked responses, and reducing functional connectivity across cortical regions.[40–42]

The goals of this study are then 2-fold: (1) to record activation of inhibitory neurons to electrical stimulation and (2) to determine how stimulation-evoked neural activity is integrated into ongoing neural circuits. To answer these questions, we applied brief bursts of high-frequency electrical stimulation at a range of amplitudes while imaging neural activity in the primary visual cortex of awake, head-fixed mice. High-frequency stimulation (25 pulses at 250 Hz) was chosen to engage inhibitory circuits (given the known suppressive effects of high-frequency stimulation).[43] Our results show that stimulation-evoked activity in awake mice followed similar patterns to those observed in anesthetized animals; however, we find in awake animals that the activity of the neuron just prior to stimulation strongly affects the amplitude of its evoked response. This interaction between pre-stimulus activity and evoked response amplitude was minimized at larger stimulation amplitudes. In excitatory neurons, high pre-stimulus activity levels tended to diminish the evoked response or even actively suppress ongoing activity, whereas in inhibitory neurons the effects were more mixed. Another major difference between excitatory and inhibitory neurons was the distinct spatial recruitment patterns observed with increasing stimulation amplitude: stronger stimulation increases the volume in which inhibitory neurons are recruited and the density with which excitatory neurons are recruited.

RESULTS

Altogether, we recorded neural activity from 6,698 neurons across five mice: 6,162 excitatory neurons and 532 inhibitory neurons. Mice were head-fixed but awake and free to run or stand still. Neural activity in layers 2/3 of the mouse visual cortex was recorded using 2-photon microscopy of the pan-neuronal calcium indicator GCaMP6s during 20 min of an electrical stimulation protocol. Inhibitory neurons were labeled with red fluorescence by crossing a Tdtomato reporter line Ai14 with the GAD2-ires-cre driver line. The *Gad2* (glutamic acid decarboxylase 2) gene encodes the enzyme primarily responsible for gamma-aminobutyric acid synthesis for synaptic release, a hallmark for inhibitory neurons of all sub-types in the mammalian brain.[44–46]

We adopted stimulation parameters known to activate neurons within rodent visual cortex,[35] changing only the range of stimulation amplitudes used. Electrical stimulation consisted of 25 biphasic cathode-leading pulses delivered at 250 Hz. Stimulation was delivered once every 10 s at one of nine possible current amplitudes (3, 5, 10, 15, 20, 25, 30, 40, or 50 μA) for 10 repetitions at each amplitude delivered in pseudo-random order, such that stimulus amplitudes differed from trial to trial (Figure 1C). Figure 1 shows the experimental procedure. Sample traces recorded from a subset of neurons during the experiment are shown in Figure S1.

Stimulation-evoked neural responses scale with stimulation amplitude

Fixed-amplitude electrical stimulation-evoked variable neural responses from trial to trial (Figure 2A). Neural responses were analyzed in two separate stages consistent with known dynamics of GCaMP6s[47]: an early stage from the time of stimulation to 580 ms to capture the early rise in fluorescent signal, and a late stage consisting of the subsequent 3.29 s to capture sustained activity and signal decay (Figure 2A), so that neural responses could be significantly modulated from baseline during the early stage, the late stage, or both (see STAR Methods: significant modulation of neural activity).

Neurons were significantly modulated by a wide range of stimulation amplitudes (Figure 2B). Of all identified excitatory neurons, a small fraction were significantly modulated at 5 μA with mixed responses—some suppression and some excitation (2.7% ± 0.2%, mean ± SEM). In contrast, inhibitory neurons were first significantly modulated by electrical stimulation at 10 μA (11.1% ± 1.3% out of all identified inhibitory neurons, mean ± SEM). However, we take this difference in the minimum threshold for activation between excitatory and inhibitory excitation to reflect the low sample size (five animals) and high variability in inhibitory neuron responses across animals rather than a true difference in the threshold for activation between excitatory and inhibitory neurons (see top panels and insets in Figures 2C and 2D). Accordingly, we found no significant difference between inhibitory and excitatory mean evoked fractions at any amplitude. The fraction of significantly modulated neurons grew with stimulation amplitude up to 40 μA, plateauing at 49% (± 2.9% SEM) for excitatory neurons and 54% (± 4% SEM) for inhibitory neurons (Figure 2C). Increasing stimulation amplitude increases number of recruited neurons.[18,22,24,35,37,48] Here, we show that this relationship holds true for both excitatory and inhibitory neurons, which are recruited at similar rates.

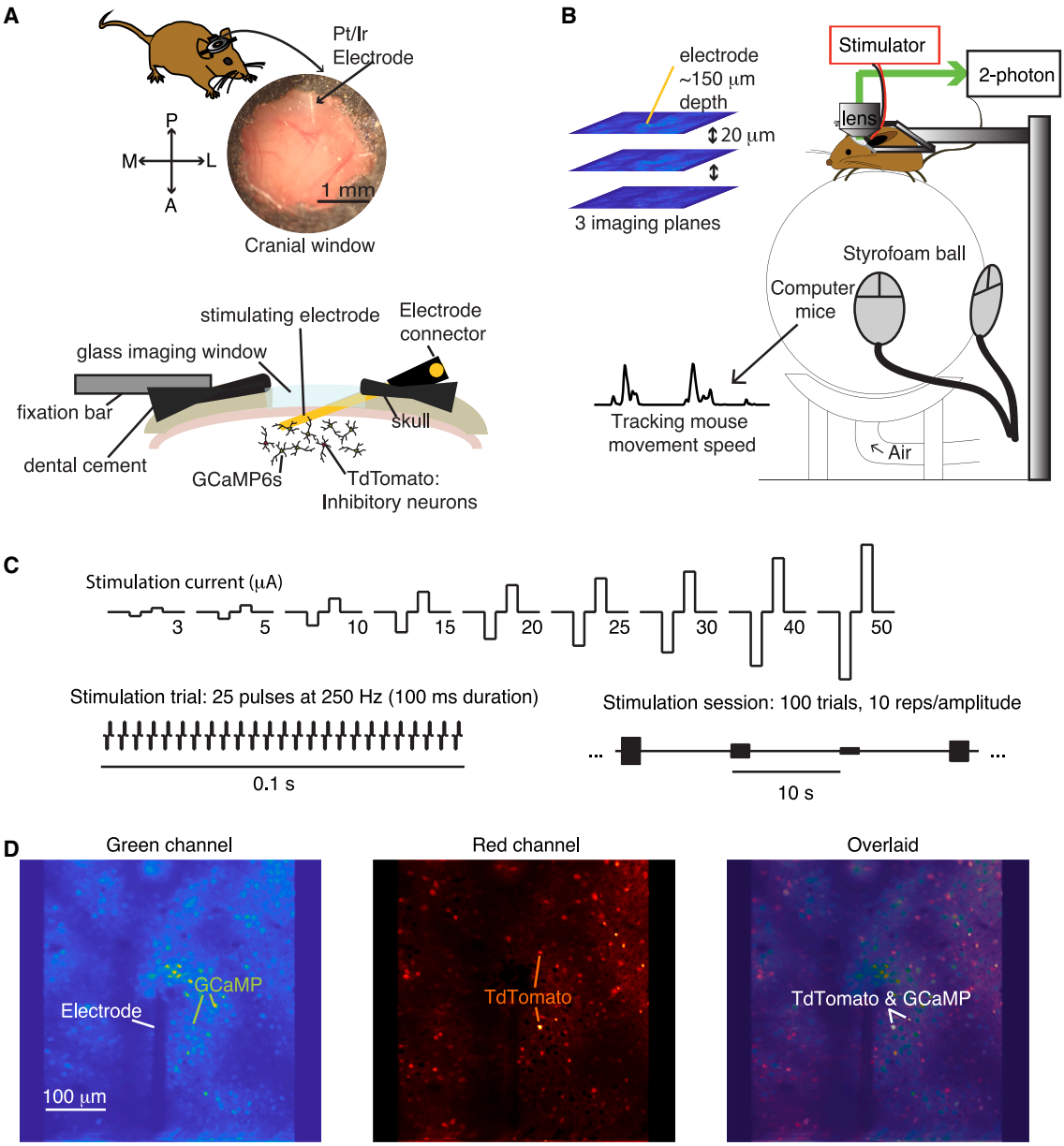

Figure 1. Neural recording and stimulation in chronically implanted awake mice

(A) A single Pt/Ir stimulating electrode was chronically implanted in mouse primary visual cortex beneath a glass imaging window.

(B) Experimental setup: awake mice are head-fixed and free to run or rest on a spherical treadmill. Three cortical planes were imaged during each imaging session.

(C) Electrical stimulation consisted of 25 biphasic cathode-leading pulses delivered at 250 Hz. Stimulation was delivered once every 10 s at one of nine possible current amplitudes: 3, 5, 10, 15, 20, 25, 30, 40, or 50 μA. Ten stimuli were delivered at each amplitude.

(D) Imaging was conducted in red and green channels to identify neurons that co-express TdTomato (inhibitory neurons) and GCamMP6s.

See also Figure S1 for sample traces from single neurons.

Moreover, increasing stimulation amplitude also increases the amplitude of stimulation-evoked neural responses (Figure 2D): defined as the maximum change in fluorescence from baseline in the 3.68 s following stimulation (ΔF). The average stimulation-evoked amplitude of excitatory neurons grew steadily until 40 μA, whereas the average stimulation-evoked amplitude of inhibitory neurons grew only until 15 μA. This difference reflects the greater variability in responses patterns across mice for inhibitory neurons than excitatory neurons. Across the range of stimulating amplitudes, there is no significant difference in evoked amplitude between excitatory and inhibitory neurons.

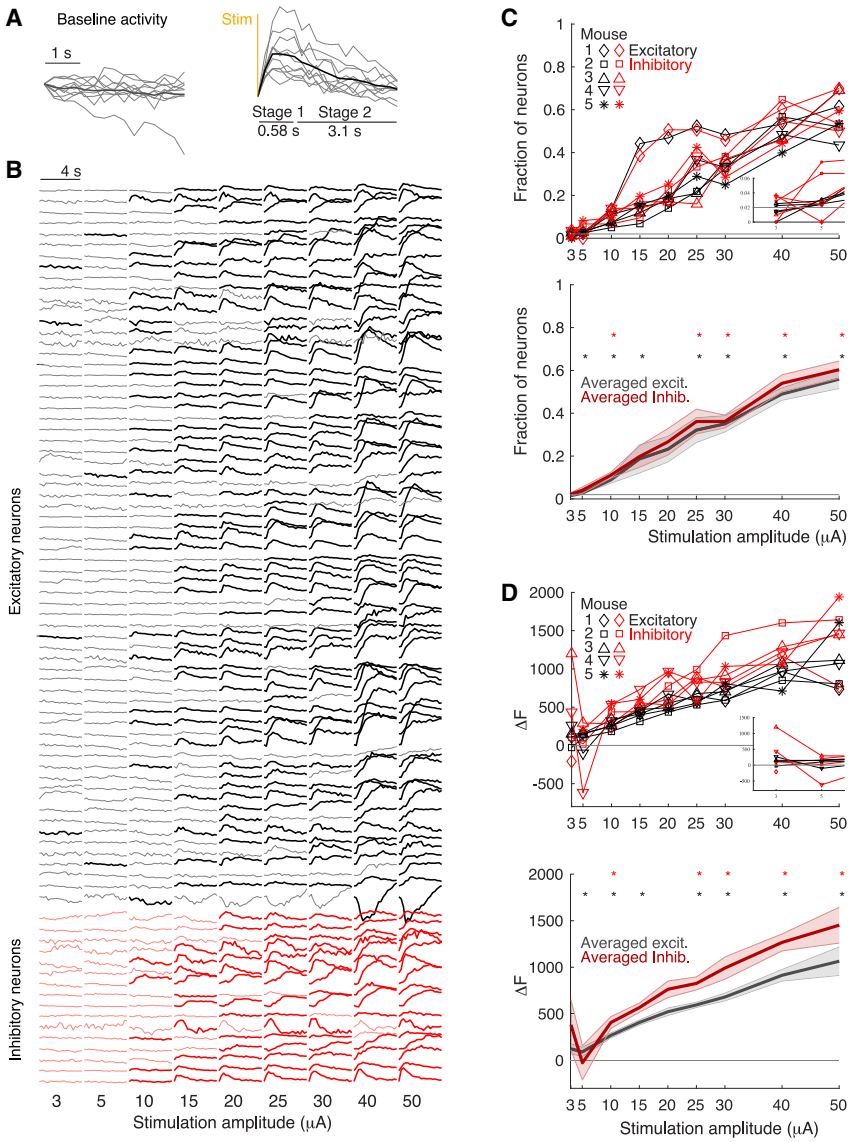

Figure 2. Stimulation-evoked neural responses by stimulation amplitude

(A) Significant stimulation-evoked responses were identified by a Wilcoxon rank-sum test comparing average single-trial evoked responses to baseline (left) with (1) stimulation onset to 800 ms following stimulation (stage 1) and (2) the subsequent 3 s (stage 2).

(B) Sample average evoked responses from a subset of mouse 1. Each row is a single neuron. Significant responses in heavy black (excitatory neurons) or red (inhibitory neurons) lines (threshold for significance set at p 0.02, Wilcoxon rank-sum test).

(C) Fraction of neurons significantly modulated by stimulation. Red shows inhibitory neurons; black shows excitatory neurons. Top: individual averages for each of the five mice. Bottom: mean and standard error across mice. Stars show significant modulation of the population ($p < 0.05$, t test, using the Holm-Bonferroni correction for multiple comparisons). Stars are color coded by neuron type.

(D) Average response amplitude relative to baseline (Δ F) of significantly modulated neurons. Top panel shows individual mice; bottom panel shows average across all mice. Shaded error bars are standard error of the mean across mice. Colors and stars as in (C).

Neurons have distinct temporal response profiles

A close examination of the neural responses in Figure 2B reveals that individual neurons have different temporal response patterns to stimulation. To better characterize neural responses to stimulation, we first classified each response from every significantly modulated neuron into one of four categories, distinguished by the timing of significant modulation in the response (early or late stage) and the sign of the response (positive or negative, indicating excitation or suppression). We found almost every possible combination of response patterns in the data (see STAR Methods) but present here four major classes: short-latency excitation, long-latency excitation, short-latency suppression, and long-latency suppression (Figure 3A). In electrophysiological recordings, directly activated action potentials are observable within 0.5 ms of stimulation, whereas transsynaptic action potential generally appear later that 0.7 ms.[18] Given the low sampling rate of 2-photon imaging and relatively slow rise time of the calcium indicator, we cannot distinguish between direct or indirect excitation of neurons by electrical stimulation during the early response period and therefore cannot map short-latency responses into direct or indirect activation of neurons. Nevertheless, we expect that the difference between short-latency and long-latency reflect distinct network activation patterns. For example, long-latency excitation may reflect a period of rebound excitation following network-induced inhibition, such as is visible in electrophysiological recordings of stimulation-evoked activity.[24]

To gain better insight into stimulation-evoked neural response patterns (Figures 3B and 3C), we calculated the number of significantly modulated neurons as a function of stimulation amplitude separately for each response pattern. Data were compiled across all five experimental animals and separated by excitatory and inhibitory neuronal types. The major response type at each stimulation amplitude was short-latency excitation (Figures 3B and 3C), growing to a maximum of 36–39% of observed inhibitory and excitatory neurons, respectively, at 50 μA.

The distribution of response profiles within the neural population varies with stimulation amplitude. At 3 μA, short-latency excitation represents 43% of significantly modulated single-neuron responses, whereas almost 50% of significantly modulated neurons were suppressed by stimulation (at short or long latency; Figure 3C). The large fraction of suppressed responses is consistent with past electrophysiological data that shows that weak stimulation primarily suppresses neural firing.[24] The

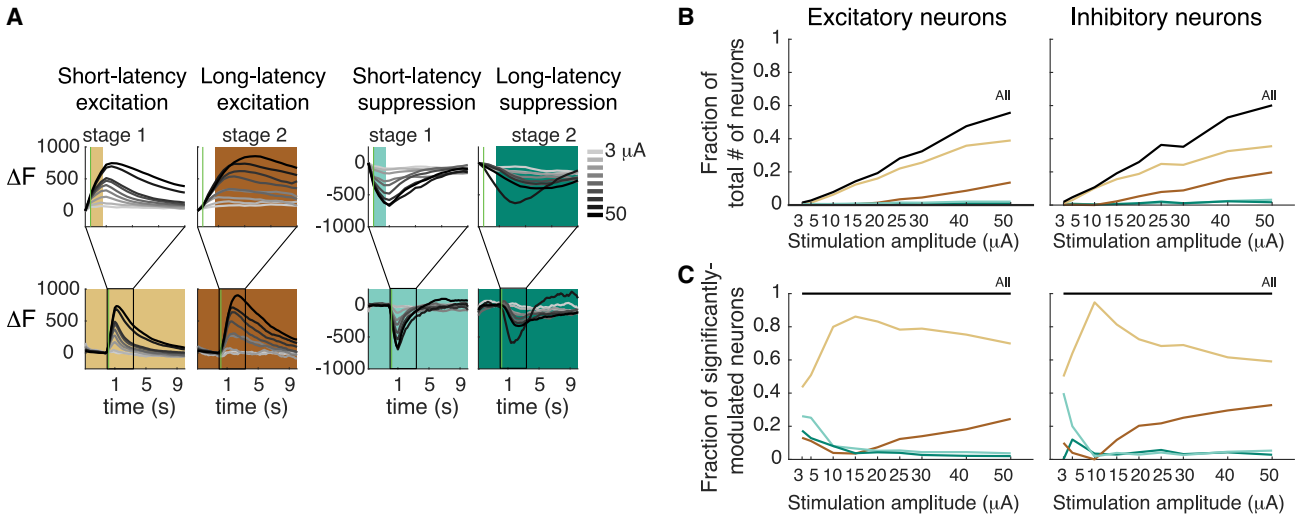

Figure 3. Distinct categories of stimulation-evoked neural responses

(A) Four classes of neural responses. Traces show the median response across all significantly modulated neurons within each category. Color-coded responses are shown for each stimulation amplitude. Time of stimulation is shown by the vertical green line.

(B) Distribution of neural response types as a function of stimulation amplitude. Data are shown as the fraction of the total number of recorded neurons that are significantly modulated by stimulation and show each type of response profile. Black lines show summed total across the response categories. Colors as in (A).

(C) Data are shown as the fraction of neurons with each response type out of the neurons that are significantly modulated at each stimulation amplitude. Lines show data compiled across five experimental animals. Colors as in (A).

mechanism by which electrical stimulation directly modulates neural activity is thought to be excitation[19,20]; therefore, the observed suppression likely results from indirect suppression by activated inhibitory neurons.[21] Suppression may dominate at low stimulation amplitudes due to the difference in excitatory and inhibitory neuron morphology. Given that the axon is depolarized during stimulation,[17–20] the level of arborization predicts which neurons are most easily activated by electrical stimulation.[49] Inhibitory neurons have denser local axonal arborizations within cortical layers 2/3 than do pyramidal cells[49] and therefore are more likely activated at low stimulation amplitudes. Furthermore, despite our observation that excitatory neurons and inhibitory neurons are recruited at similar rates, there is some evidence that stimulation antidromically activates neural cell bodies at lower rates than the projecting neural axons,[43] which implies that recording cell bodies underestimates inhibitory neuron activation. Therefore, we propose that the locally dense inhibitory neuron axons are preferentially recruited at low stimulation amplitudes, leading to the observed suppression of neural responses.

Inhibition may be overcome with increasing stimulation amplitude because the greater current spread activates a larger fraction of neurons. Indeed, approximately 80% of evoked neural responses at 15 μA show short-latency excitation. Beyond 15 μA, the fraction of responses having short-latency excitation gently falls to 60%–70% by 50 μA (Figure 3C). In contrast, long-latency excitation, likely reflecting indirect exciton of neural activity, steadily grows with stimulation amplitude, peaking at 24%–33% by 50 μA (Figure 3C). The long-latency responses may come from larger response amplitudes of primary-activated neurons at high-stimulation amplitudes (Figure 3A), which robustly activate the neural circuit, increasing both transynaptic transmission and rebound responses following inhibition.[35,50]

Spatial distribution of stimulation-evoked neural responses

We next analyzed the spatial relationship between stimulation amplitude and significant stimulation-evoked responses (Figure 4). To qualitatively assess this relationship, we plot the location of significantly modulated neurons relative to the electrode tip for one mouse (Figure 4A), color-coding each neuron by its response class. Activation patterns for the other four mice are shown in Figure S2. These plots show that stimulation-evoked activity expanded to the edge of our field of view by 20 μA. Therefore, we consider changes in the volume and density of stimulation-evoked activity only up to 20 μA. Volume is calculated by drawing a boundary around the three-dimensional space taken up by activated neurons, which allows for asymmetric activation. The result is also presented using the conventional radial measure of neural activation in Figure S3.

Consistent with prior work,[22,35] we found that the three-dimensional (3D) volume of space taken up by significantly modulated neural cell bodies did not significantly increase with stimulation amplitude for excitatory neurons, and only at 15 μA had it increased significantly for inhibitory neurons (tests for significance compared with response distribution at 3 μA; Figure 4B). The density of significantly activated excitatory neurons grew more sharply, reaching significant difference by 10 μA (tests for significance compared with response distribution at 3 μA; Figure 4C). In contrast to excitatory neurons, the density of significantly modulated inhibitory neurons did not change with stimulation amplitude (Figure 4C).

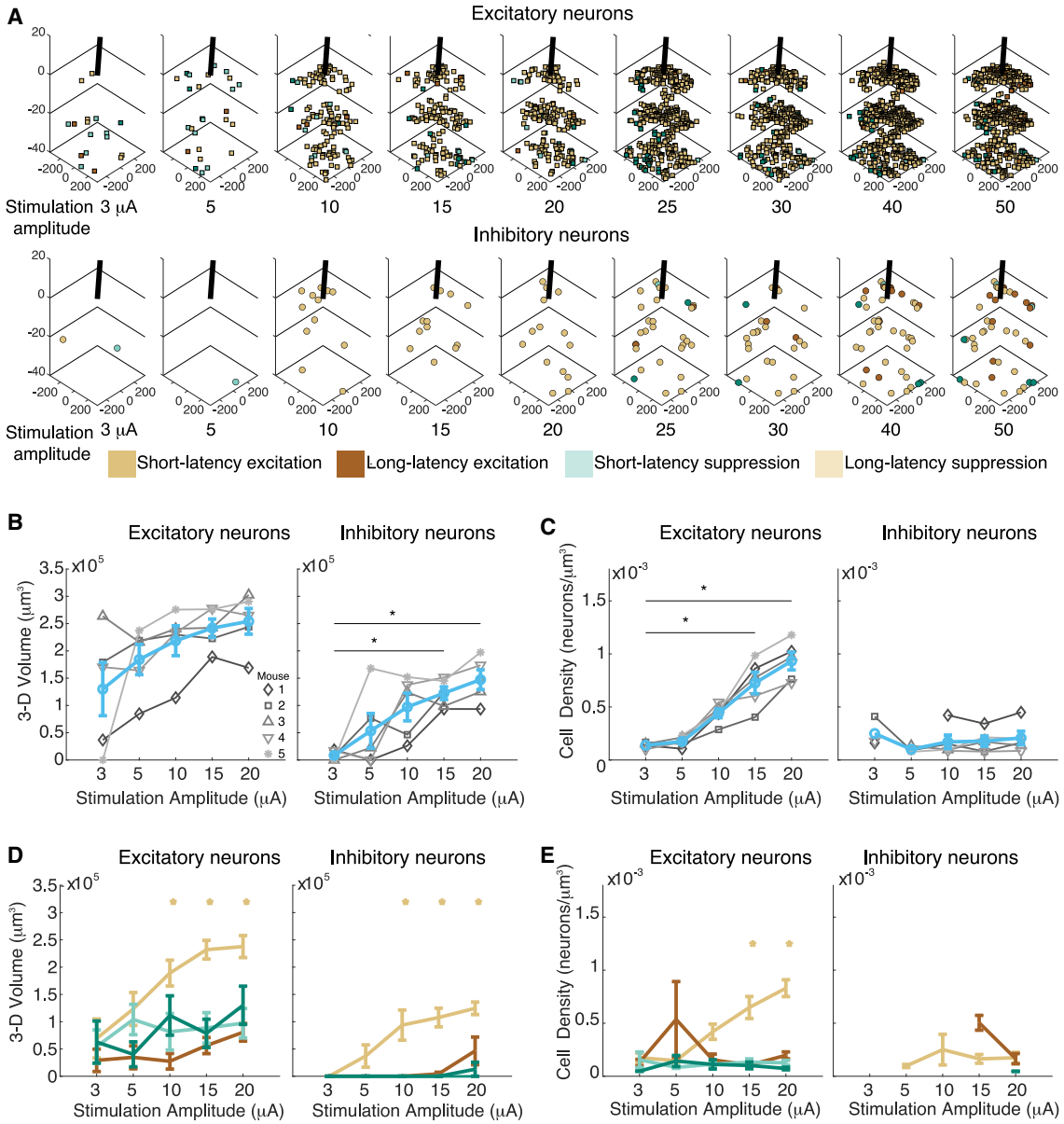

Figure 4. Spatial distribution of stimulation-evoked neural responses as a function of stimulation amplitude

(A) Spatial distribution of responses as a function of stimulation amplitude for excitatory neurons (top) and inhibitory neurons (bottom) from a single experimental animal (mouse 1). The black line shows the stimulating electrode. Three stacked imaging planes are shown, each 20 μm apart. Axis coordinates show distance from the electrode tip in μm. Each marker represents the location of a neuron that was significantly modulated by stimulation. The marker color shows a neuron's average response. See also Figure S2 for spatial distribution of responses from the remaining experimental animals.

(B) The the 3D volume of space covered by significantly modulated neurons at each stimulation amplitude, calculated as the outer boundary of all the neuron locations. Significant changes in volume from the value at 3 μA are indicated as $*$ symbol ($p < 0.05$, two-sample t test, Holm-Bonferroni correction for multiple comparisons). See also Figure S3 for a measure of the average radial distance at which neuron responded to stimulation.

(C) The density of significantly modulated neurons within the spatial volume covered by significantly modulated neurons. Significant changes in density from the value at 3 μA are indicated by stars as in (B)

(D) The 3D volume of space covered by significantly modulated neurons at each stimulation amplitude. Colors represent different response profiles, color-coded as in (A). Significant changes in volume from the value at 3 μA are indicated by the $*$ symbol ($p < 0.05$, two-sample t test, Holm-Bonferroni correction for multiple comparisons).

(E) The density of significantly modulated neurons within the spatial volume covered by significantly modulated neurons at each stimulation amplitude. Data are broken categories as in (A). Significant changes in density from the value at 3 μA are indicated by stars as in (D).

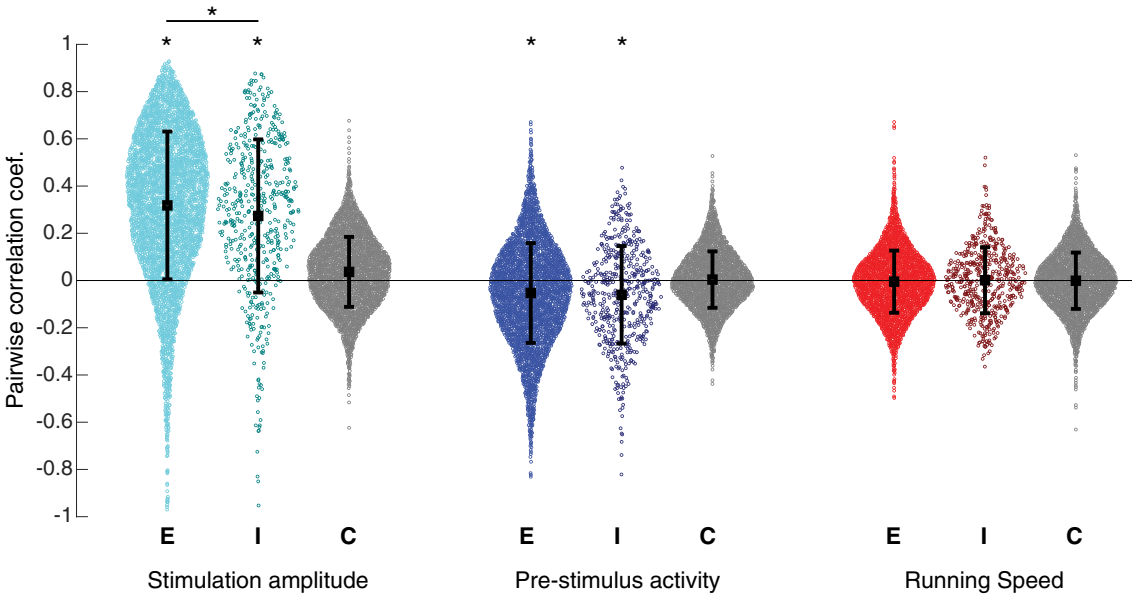

Figure 5. Correlation between stimulation-evoked responses and experimental variables

Correlation between stimulation-evoked responses and experimental variables. Cell-type-specific correlations between the amplitude of stimulation-evoked responses (ΔF) and stimulation amplitude, pre-stimulus activity, and running speed. Each circle denotes a single cell; data were compiled from all neurons in all mice. E indicates excitatory neurons, I indicates inhibitory neurons, and C is the control condition (both excitatory and inhibitory neurons) where data were shuffled across trials. Stars above each distribution denote a significant difference relative to controls or differences between excitatory and inhibitory populations ($p < 0.01$, Wilcoxon rank-sum test).

The difference in changes in density with increasing stimulation amplitude between excitatory and inhibitory neurons suggests different mechanisms of recruitment. Excitatory neurons are sparse and distributed throughout the space, and increasing current amplitude adds more neurons to the same volume, increasing the observed density. In contrast, inhibitory neuron recruitment can maintain the same average density across stimulation amplitude if they are recruited within a sphere surrounding the electrode tip whose volume grows with increasing amplitude, such that additional neurons are recruiting from a larger volume. The increase in average volume and density with stimulation amplitude was being driven primarily by changes in the spatial distribution of short-latency excitation (Figures 4D and 4E), which matched the changes observed in the overall population. For excitatory neurons, there was no average change in volume or density of the other response types; however, the difference may be due to the relatively smaller sample size of the other response types. For inhibitory neurons, the sample size of neurons with response profiles other than short-latency excitation were sparse (Figure 3), which made for noisy estimates of volume and density split by response type.

Modulation of stimulation-evoked responses by ongoing neural activity

The responses of single neurons to electrical stimulation were variable across repeated stimulation trials with a fixed stimulation amplitude (Figure 5A). This variability could be due to fluctuations in the underlying neural activity patterns at the time of stimulation that modulate stimulus-driven responses as a function of motor behavior, locomotion, or cortical state.[27,51–53]

To determine the factors that contribute to variability in stimulation-evoked responses, we calculated the pairwise correlation between each neuron's single-trial early stage responses to stimulation with three variables: (1) electrical stimulation amplitude, (2) the animal's running speed during stimulation, and (3) each neuron's pre-stimulus activity level (the mean activity in the 1 s prior to stimulation onset). We found that stimulation amplitude and pre-stimulus activity affect stimulation-evoked responses (Figure 5B). As expected from a prior analysis (Figure 2D), stimulation amplitude had a positive average correlation with the amplitude of evoked neuronal responses: 0.32 ± 0.31 (mean ± standard deviation) for excitatory neurons and 0.27 ± 0.32 for inhibitory neurons. In addition, the average correlation coefficient for excitatory neurons was significantly higher than the average correlation coefficient for inhibitory neurons ($p = 0.001$, Wilcoxon rank-sum test). Therefore, the stimulation-evoked responses of excitatory neurons more closely follow stimulation amplitude than the responses of inhibitory neurons.

In contrast to the positive correlations observed with stimulation amplitude, pre-stimulus neural activity was negatively correlated with stimulation-evoked responses, suggesting that stimulation tended to suppress or diminish ongoing neural activity (Figure 5B): −0.05 ± 0.21 (mean ± standard deviation) for excitatory neurons and −0.06 ± 0.21 for inhibitory neurons, both significantly different from the control (shuffled trial labels; $p \leq 0.0001$, Wilcoxon rank-sum test). There was no significant difference between the distribution of correlation coefficients for inhibitory and excitatory neurons ($p = 0.43$, Wilcoxon rank-sum test). Unlike stimulation amplitude and pre-stimulus activity, the animal's running speed at the

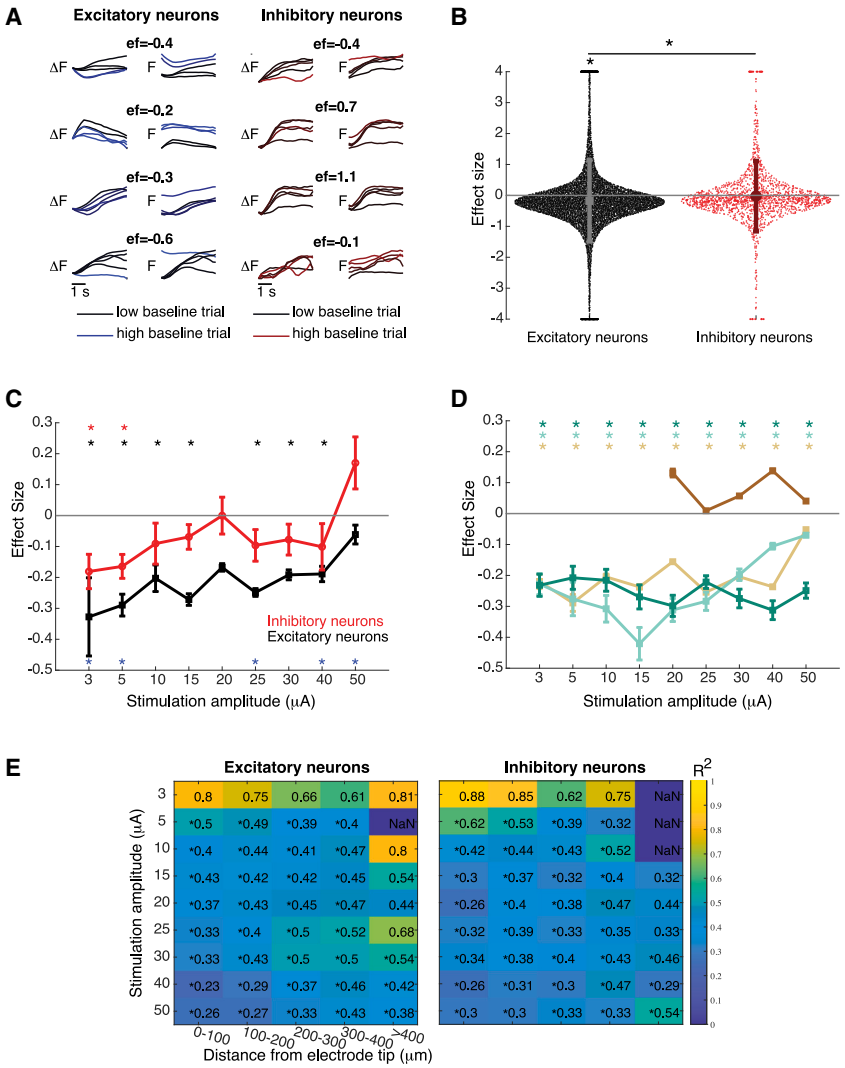

Figure 6. Variability in stimulation-evoked responses can be explained by pre-stimulus activity

(A) Example evoked responses to electrical stimulation at 50 μ A for excitatory and inhibitory neurons (F: raw fluorescence, Δ F: aligned to timepoint just prior to stimulation). These responses are shown in arbitrary units, which cannot be compared across neurons. The color of each single-trial response reflects the relative amplitude of the pre-stimulus activity, with lighter colors (blue and red) indicating higher pre-stimulus activity levels. Above each neuron is a calculated effect size across trials (ef). Only trials that did not follow high-amplitude stimulation are shown.

(B) Effect size distribution, mean, and standard error (overlaid) for significantly modulated excitatory neurons (black) and inhibitory neurons (red) at all stimulation amplitudes. Stars indicate a significant difference from mean zero ($p < 0.05$, t test) or significant difference between excitatory and inhibitory neurns ($p < 0.05$, Wilcoxon rank-sum test).

(C) Effect size mean and standard error plotted as a function of stimulation amplitude, separately for excitatory (black) and inhibitory (red) neurons that were significantly modulated by electrical stimulation. Significant difference from zero is indicated by red and black stars ($p < 0.05$, Wilcoxon sign-rank test, using the Holm-Bonferroni correction for multiple comparisons within each neuron class). Significant differences between neuron types are indicated by blue stars (excitatory vs. inhibitory; $p < 0.05$,Wilcoxon rank-sum test, using the Holm-Bonferroni correction for multiple comparisons).

(D) The mean and standard error for effect size plotted as a function of stimulation amplitude, separately for each response type. Significant difference from zero is indicated by color-coded stars ($p < 0.05$, Wilcoxon sign-rank test, using the Holm-Bonferroni correction for multiple comparisons within each neuron class). Data points with fewer than 30 neurons were excluded from the figure.

(E) The fraction of the variance in stimulus-evoked responses that is explained by the value of pre-stimulus activity (i.e., the R^2 value of the linear regression show in A), averaged across neurons significantly modulated at each stimulation amplitude (vertical axis) and at each distance from the stimulating electrode (horizontal axis). Stars denote significant difference from the R^2 values at 3 μ A within 0–100 μ m of the electrode tip ($p < 0.05$, Wilcoxon rank-sum test, using the Holm-Bonferroni correction for multiple comparisons within each class of neurons).

time of stimulation was uncorrelated with the amplitude of stimulation-evoked neural activity ($\rho_{excitatory}$ = −0.005 ± 0.13 and $\rho_{inhibitory}$ = 0.001 ± 0.14; Wilcoxon rank-sum test; Figure 5B).

To quantify the relationship between pre-stimulus activity and evoked response amplitude at each stimulation amplitude, "effect size" was calculated as the slope of the linear regression between the trial-by-trial stimulation-evoked responses of a neuron and its corresponding pre-stimulus activity (Figure 6). A negative effect size indicates that high pre-stimulus activity suppresses or diminishes stimulation-evoked responses, and a positive one indicates that high pre-stimulus activity facilitates stimulation-evoked responses. A near-zero effect size indicates no consistent effect of pre-stimulus activity on evoked responses across trials.

Effect sizes were variable across the population of recorded neurons (Figure 6B). Excitatory neurons had a significantly lower average effect size than did inhibitory neurons (−0.14 ± 1.41 vs. 0.02 ± 1.19; Figure 6A). For a more detailed view, we plotted effect sizes separately at each stimulation amplitude and found that effect sizes grew weaker with increasing amplitude (Figure 6B). Inhibitory neural responses evoked by stimulation were, on average, diminished only at low-amplitude stimulation (3 and 5 μA). In contrast, excitatory neuron responses to stimulation were significantly diminished up until 50 μA.

Splitting the neural population by stimulation-evoked response types reveals that pre-stimulus activity has different relationships with each response type (Figure 6D). The most prominent change is that the amplitude of long-latency excitatory responses is facilitated by high pre-stimulus activity. In contrast, both short- and long-latency suppression have negative effect sizes at all stimulation amplitudes. Short-latency excitatory responses, which

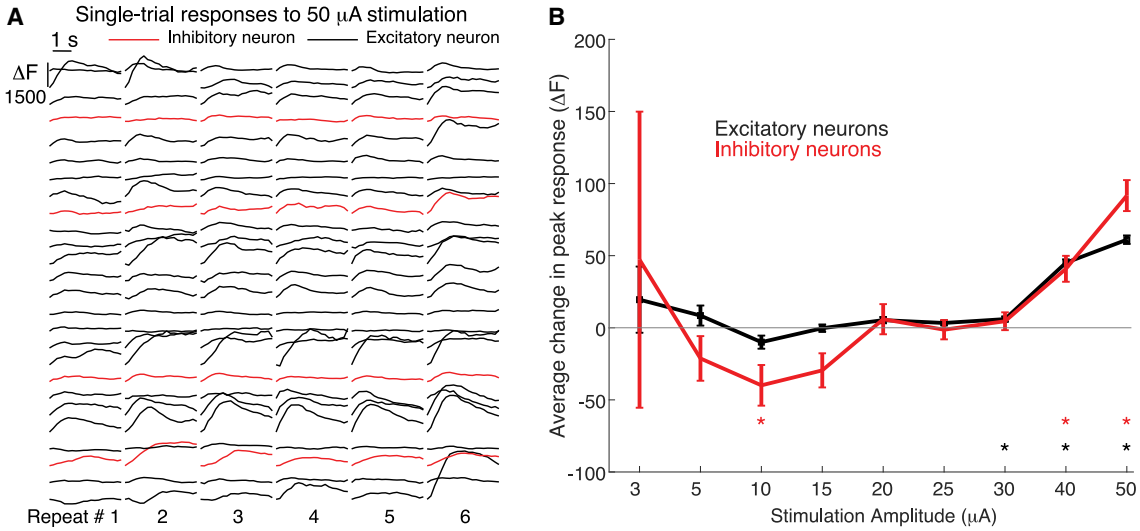

Figure 7. The effect of repeated stimulation on evoked activity patterns

(A) Evoked responses to stimulation trials at 50 μA of a subset of significantly modulated neurons are shown for each repeat of a stimulation trial that did not follow a high-amplitude stimulation trial (defined as 30, 40, or 50 μA). Colors indicate neuron type (inhibitory vs. excitatory). Responses have been smoothed for clarity. (B) The "repeat effect" (i.e., the slope of the linear relationship between the amplitude of single-trial stimulation-evoked responses and the trial number) for inhibitory neurons (red) and excitatory neurons (black) that were significantly modulated by stimulation at each amplitude. Lines show mean and standard error. Stars indicate significant difference (i.e., rejecting the null hypothesis of zero change in evoked amplitude across repeated stimulation trials) for excitatory (black) and inhibitory (red) neurons ($p < 0.05$, t test, Holm-Bonferroni correction for multiple comparisons).

compose the majority of responses at all stimulation amplitudes (Figure 3), gradually decrease in effect-size amplitude with increasing stimulation amplitude.

Finally, to quantify how well the pre-stimulus fluctuations can predict the variance of the stimulation-evoked responses, we calculated the R^2 value of the regression model for each neuron under different stimulation amplitude. We binned inhibitory and excitatory neurons by their radial distance from the electrode tip and calculated the average R^2 in each bin as a function of stimulation amplitude (Figure 6E). We found a strong interaction between stimulation amplitude, radial distance, and effect size. Pre-stimulus baseline activity strongly modulates the response evoked by low-amplitude stimulation; however, the relationship is much weaker at higher stimulation amplitudes. Additionally, moving further away from the electrode tip has the effect of weakening the electrical current that is seen by neural cell bodies and processes, and pre-stimulus baseline activity has a stronger influence, as evidenced by larger R^2 values at greater distances. These results paint an interesting picture regarding the ability to use electrical stimulation to manipulate neural activity patterns. Strong stimulation can control neural activity within a small region surrounding the electrode tip but leads to variable results in a larger region surrounding the site of stimulation, where stimulation is integrated into ongoing activity patterns of neural circuits.

Neural responses adapt to repeated stimulation

Prolonged periods of stimulation can drive neural plasticity.[54,55] Here, we found that repeated stimulation did indeed modulate the effect of repeated stimulation dependent on the amplitude of stimulation as well as on neuron type (Figure 7). To test for short-term depression in stimulation-evoked responses, we calculated a "repeat effect size" by regressing the mean stimulus-evoked response on each trial against trial number and using the slope of the regression line as the measure of the effect of repeated stimulation. Inhibitory neuron responses at high-stimulation amplitudes were facilitated by repeated stimulation and were moderately suppressed at 20 μA but showed no significant changes at lower stimulation amplitudes. Repeated stimulation of excitatory neurons at high amplitudes were similarly facilitated (20–50 μA), with stronger responses appearing across trials; however, repeated stimulation at 10 μA led to significant suppression across trials.

DISCUSSION

In this study, we applied two-photon imaging combined with cell-type-specific labeling to address an outstanding scientific question: how does electrical stimulation affect cortical inhibitory neurons? Prior work had only indirectly measured the contribution of inhibition to network responses to electrical stimulation and was largely conducted in anesthetized animals.

There are three major classes of inhibitory interneurons that make up 10%–20% of neurons in the brain: parvalbumin (PV)-expressing, somatostatin (SST)-expressing, and vasoactive intestinal peptide (VIP)-expressing neurons. Each of the three classes has distinct connections with one another and with excitatory neurons and thus serves a separate function within the cortical circuit[56–58]; therefore, modulating each class will have a different effect on neural processing.[59,60] For example, PV neurons regulate spatiotemporal patterns of activity,[61] whereas VIP neurons disinhibit sensory-evoked responses in excitatory neurons.[62] Although in this manuscript we do not differentiate between

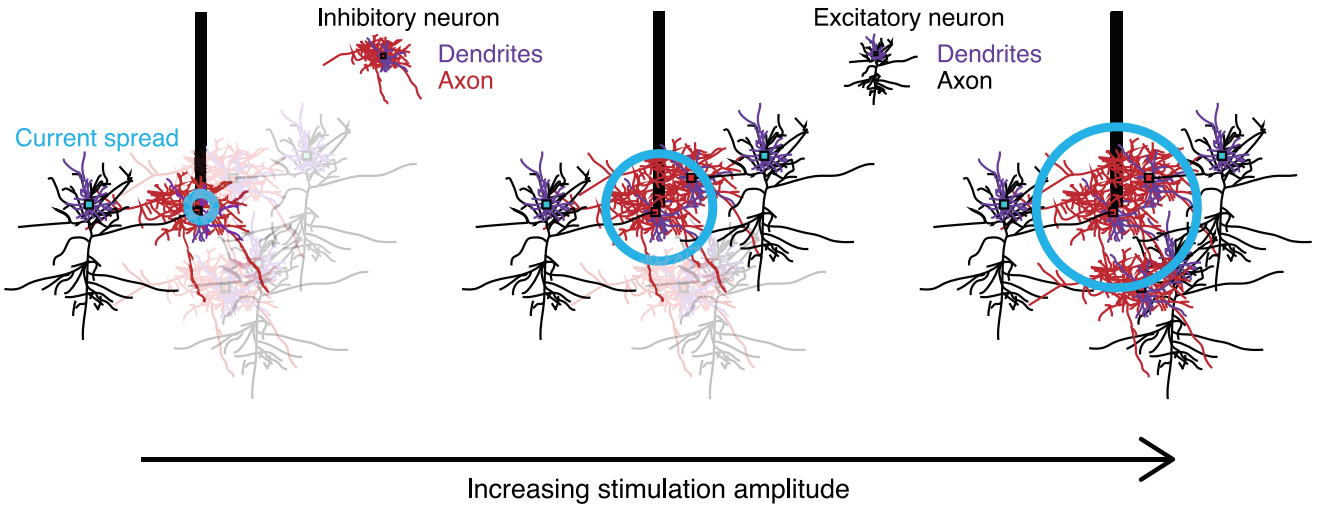

Figure 8. Differential spatial patterns of recruitment for inhibitory and excitatory neurons

Differential spatial patterns of recruitment for inhibitory and excitatory neurons as stimulation amplitude increases: excitatory neurons increase density within a fixed volume, whereas inhibitory neurons remain at fixed density while activation volume increases. Neurons that are significantly modulated by stimulation are shown in dark colors. Neural cell bodies (soma) are shown as filled square (cyan for excitatory neurons, red for inhibitory neurons). The dendrites of each cell are shown in purple, and axons are shown in black for excitatory neurons and red for inhibitory neurons. The neural morphology shown is based on reconstructions of anatomical data presented in Komarov et al.[49]

the three classes of inhibitory neurons, we validate a genetic approach to distinguish the effects of electrical stimulation on excitatory and inhibitory neural populations by taking advantage of transgenic mouse lines. We found both similarities (recruitment rates, temporal response profiles, and potentiation from repeated stimulation) and differences (spatial recruitment pattern and dependence on pre-stimulus activity) between recruitment of excitatory and inhibitory neurons by electrical stimulation. Our results underscore the need to further characterize neural responses in a subtype-specific manner.

Excitatory vs. inhibitory neuron recruitment by electrical stimulation

Similar to prior work in anesthetized animals,[16,35,48,50] we found that the number and amplitude of stimulation-evoked neuronal responses scale with stimulation amplitude. Furthermore, the recruitment of excitatory and inhibitory neurons grows with stimulation amplitude at approximately the same rate (Figure 2). These results agree with contemporary work that indirectly inferred neuron class[33] but contradicts computational models that predict that stimulation would recruit a somewhat larger fraction of excitatory neurons than inhibitory neurons.[22,63] The difference may be explained by the nature of evoked responses considered by the experimental vs. computational work: the models predict direct activation of neurons by stimulation, whereas the experimental work additionally includes indirectly activated neurons. Indirect activation of inhibitory neurons following stimulation via strong projections from excitatory neurons[58] may approximately equalize the fractions of the recruited inhibitory and excitatory population.

In contrast to similar rates of recruitment, excitatory and inhibitory neurons were activated with distinct spatial patterns: increasing stimulation amplitude recruits excitatory neurons in a fixed volume with increasing density but recruits inhibitory neurons with increasing volume and fixed density (Figure 4). This observation mirrors computational predictions that interneuron recruitment is dense around the electrode, whereas excitatory neuron recruitment is sparse and distributed.[63] These distinct recruitment patterns, in turn, dictate the distinct spatial distributions of recruited neurons described above (Figure 8). For excitatory neurons, increasing current amplitude adds more neurons to the same volume, yielding higher activation density. In contrast, inhibitory neurons are activated within a sphere surrounding the electrode tip; increasing amplitude then recruits more neurons from a larger area, maintaining approximately the same activation density.

Our data consisted of fewer inhibitory neurons than expected for the upper layers of rodent cortex—just 8% of recorded neurons (6,162 excitatory neurons and 532 inhibitory neurons). In contrast, there are thought to be approximately $12.7 \pm 2.2\%$ in layer 2/3 of the rat primary visual cortex[64] and 11%–16% of layer 2/3 neurons in mouse barrel cortex.[65] We attribute the difference to two factors: incomplete labeling efficacy in our mouse line[44] and aggressive artifact correction in the red imaging channel used to identify inhibitory neurons (see STAR Methods: identification of inhibitory neurons).

Integration of stimulation into ongoing neural activity

Traditionally, stimulation was used to link neural activity within brain areas to sensory perception, motor functions, and other behaviors; the idea was that stimulation could activate or disrupt neural activity within a brain area, respectively, facilitating or interrupting the function of that brain area. Neural stimulation was thought to "hijack" the brain—eliminating and replacing ongoing neural activity in the target brain region.[66,67] However, the true relationship between stimulation and ongoing neural activity is more complex.

Integration of electrical stimulation into ongoing neural activity patterns has been observed across spatial scales. At the level of whole brain areas, anesthesia, arousal, and resting-state functional connectivity in brain networks all alter the effects of electrical stimulation.[68–70] At the level of single neurons, focal attention has been found to promote neural activation and signal propagation across brain areas following electrical stimulation,[28] whereas motor behavior reduces the oscillations in local field potential normally induced by stimulation.[27,30] The amplitude of local field potentials at the time of stimulation also alters the effect of stimulation, with local depolarization facilitating stimulation-evoked responses[71] and spontaneous firing rates are correlated with the probability that that a stimulus pulse elicits an action potential from a nearby neuron.[33] Furthermore, longer periods of inactivity in a neuron are associated with larger stimulus-evoked responses.[72]

In this study, we examined the integration of cortical electrical stimulation into the ongoing activity of excitatory vs. inhibitory neurons. We found that inhibitory neuron responses to stimulation are less dependent on pre-stimulus activity than are excitatory neuron responses (Figures 6B and 6C), in that they are less correlated with stimulation amplitude (Figure 5) and are less likely to have ongoing neural activity suppress stimulation-evoked responses (Figures 6B and 6C). Therefore, although inhibitory neuron responses to stimulation are well explained by pre-stimulus baselines (Figure 6E), they have a different relationship with pre-stimulus activity.

Our results notably differ from recent work that examined the effect of spontaneous firing rates on the probability that a single pulse of stimulation would elicit an action potential.[33] In that study, electrophysiological recordings were made of neural responses to single-pulse stimulation. The authors found that the probability a spike would be elicited was highly correlated to the neuron's spontaneous firing rate. In contrast, we find that excitatory neuron responses to stimulation are, on average, suppressed by stimulation. We propose that the difference between our studies is the method of stimulation used: single pulse vs. high-frequency multi-pulse. Although ongoing neural activity facilitates responses to single-pulse stimulation, ongoing neural activity suppresses responses to high-frequency multi-pulse stimulation. Clearly, high-frequency stimulation activates inhibitory networks within the cortex during periods of high activity. In contrast, single-pulse stimulation activates circuits that facilities neural spiking. Taken together, these two studies emphasize the interaction between stimulus parameters and ongoing networks of neural activity.

Implications for neural prostheses

Beyond a technical analysis of stimulation-evoked neural activity within the cortex, our work has implications for neural prostheses, particularly thinking about encoding artificial sensory information within neural circuits. The goal of providing artificial sensation is to replace a lost sensation, which requires patterned modulation of neural activity within the periphery, thalamus, or one of the sensory cortices.[9,11,73–77] Clearly, electrical stimulation is capable of modulating neural activity patterns in the brain, and, beyond its clinical viability, it is readily detectable by animals and humans alike.[1,9,11,78] But the target of electrical stimulation matters. Activating a single putative inhibitory neuron elicits a stronger but more variable percept than activating single putative excitatory neuron.[23] If strong activation is ideal, then clearly inhibitory neurons should be targeted. On the other hand, stable evoked patterns of neural activity are easier to learn than those that are more variable.[79] Thus, targeting excitatory neurons alone or in combination with a stimulation patterns that activates SST neurons (the activity of which improves reliability of neural spiking[60]) could improve artificial sensation. From the work in this paper, we can additionally suggest that increasing stimulation amplitude to certain extent (beyond 15 μA in the mouse visual cortex) could improve stability of evoked responses by reducing their dependence on ongoing activity patterns in the brain, which should help learning and integration of artificial sensory signals into natural sensorimotor function.[80]

STAR★METHODS

Detailed methods are provided in the online version of this paper and include the following:

- KEY RESOURCES TABLE
- RESOURCE AVAILABILITY
  - Lead contact
  - Materials availability
  - Data and code availability
- METHOD DETAILS
  - Surgery
  - Electrical stimulation
  - Two-photon calcium imaging
- QUANTIFICATION AND STATISTICAL ANALYSIS
  - Registration, cell detection, and neuropil correction
  - Identification of inhibitory neurons
  - Radial distance from electrode tip
  - 3D Volume from electrode tip
  - Significant modulation of neural activity
  - Removal of data following high-amplitude trials
  - Amplitude and variance of evoked neural responses
  - Establishing neural response profiles
  - Neural correlations and Effect size

SUPPLEMENTAL INFORMATION

Supplemental information can be found online at https://doi.org/10.1016/j.neuron.2023.11.022.

ACKNOWLEDGMENTS

The work completed in this article was supported by NIH grant EY02874, UCSF Program in Breakthrough Biomedical Research, NSF HDR grant 2117997, and the Ralph W. and Grace M. Showalter Research Trust. M.P.S. was a recipient of the RPB Disney Award for Amblyopia Research.

AUTHOR CONTRIBUTIONS

M.C.D., Y.J.S., and M.P.S. designed the study and wrote the manuscript. M.C.D. and Y.J.S. performed the experiments and analyzed the data.

DECLARATION OF INTERESTS

The authors declare no competing interests.

Received: November 17, 2022
Revised: August 4, 2023
Accepted: November 22, 2023
Published: December 21, 2023

REFERENCES

1. Penfield, W., and Perot, P. (1963). The brain's record of auditory and visual experience: a final summary and discussion. Brain *86*, 595–696.
2. Histed, M.H., Ni, A.M., and Maunsell, J.H.R. (2013). Insights into cortical mechanisms of behavior from microstimulation experimetns. Prog. Neurobiol. *103*, 115–130.
3. Cohen, M.R., and Newsome, W.T. (2004). What electrical microstimulation has revealed about the neural basis of cognition. Curr. Opin. Neurobiol. *14*, 169–177.
4. Musk, E. (2019). An integrated brain-machine interface platform with thousands of channels. J. Med. Internet Res. *21*, e16194.
5. Ho, E., Hettick, M., Papageorgiou, D., Poole, A.J., Monge, M., et al. (2022). The Layer 7 cortical interface: a scalable and minimally invasive brain–computer interface. bioRxiv.
6. Lycke, R., Kim, R., Zolotavin, P., Montes, J., Sun, Y., Koszeghy, A., Altun, E., Noble, B., Yin, R., He, F., et al. (2023). Low-threshold, high-resolution, chronically stable intracortical microstimulation by ultraflexible electrodes. Cell Rep. *42*, 112554.
7. Armenta Salas, M., Bashford, L., Kellis, S., Jafari, M., Jo, Hyeongchan, Kramer, D., Shanfield, K., Pejsa, K., Lee, B., Liu, C.Y., et al. (2018). Proprioceptive and cutaneous sensations in humans elicited by intracortical microstimulation. eLife *7*, 1–11.
8. Tabot, G.A., Dammann, J.F., Berg, J.A., Tenore, F.V., Boback, J.L., Vogelstein, R.J., and Bensmaia, S.J. (2013). Restoring the sense of touch with a prosthetic hand through a brain interface. Proc. Natl. Acad. Sci. USA *110*, 18279–18284.
9. Flesher, S.N., Collinger, J.L., Foldes, S.T., Weiss, J.M., Downey, J.E., Tyler-Kabara, E.C., Bensmaia, S.J., Schwartz, A.B., Boninger, M.L., and Gaunt, R.A. (2016). Intracortical microstimulation of human somatosensory cortex. Sci. Transl. Med. *8*, 361ra141.
10. Callier, T., Brantly, N.W., Caravelli, A., and Bensmaia, S.J. (2020). The frequency of cortical microstimulation shapes artificial touch. Proc. Natl. Acad. Sci. USA *117*, 1191–1200.
11. Hughes, C.L., Flesher, S.N., Weiss, J.M., Boninger, M., Collinger, J.L., and Gaunt, R.A. (2021). Perception of microstimulation frequency in human somatosensory cortex. eLife *10*, 1–19.
12. Stieger, K.C., Eles, J.R., Ludwig, K.A., and Kozai, T.D.Y. (2020). In vivo microstimulation with cathodic and anodic asymmetric waveforms modulates spatiotemporal calcium dynamics in cortical neuropil and pyramidal neurons of male mice. J. Neurosci. Res. *98*, 2072–2095.
13. Eles, J.R., Stieger, K.C., and Kozai, T.D.Y. (2021). The temporal pattern of intracortical microstimulation pulses elicits distinct temporal and spatial recruitment of cortical neuropil and neurons. J. Neural Eng. *18*, 18.1.
14. McIntyre, C.C., and Grill, W.M. (2002). Extracellular stimulation of central neurons: influence of stimulus waveform and frequency on neuronal output. J. Neurophysiol. *88*, 1592–1604.
15. Michelson, N.J., Eles, J.R., Vazquez, A.L., Ludwig, K.A., and Kozai, T.D.Y. (2019). Calcium activation of cortical neurons by continuous electrical stimulation: frequency dependence, temporal fidelity, and activation density. J. Neurosci. Res. *97*, 620–638.
16. Hughes, C., and Kozai, T. (2023). Dynamic amplitude modulation of microstimulation evokes biomimetic onset and offset transients and reduces depression of evoked calcium responses in sensory cortices. Brain Stimul. *16*, 939–965.
17. Ranck, J.B. (1975). Which elements are excited in electrical stimulation of mammalian central nervous system: a review. Brain Res. *98*, 417–440.
18. Gustafsson, B., and Jankowska, E. (1976). Direct and indirect activation of nerve cells by electrical pulses applied extracellularly. J. Physiol. *258*, 33–61.
19. McIntyre, C.C., and Grill, W.M. (1999). Excitation of central nervous system neurons by nonuniform electric fields. Biophys. J. *76*, 878–888.
20. McIntyre, C.C., and Grill, W.M. (2000). Selective microstimulation of central nervous system neurons. Ann. Biomed. Eng. *28*, 219–233.
21. Hussin, A.T., Boychuk, J.A., Brown, A.R., Pittman, Q.J., and Teskey, G.C. (2015). Intracortical microstimulation (ICMS) activates motor cortex layer 5 pyramidal neurons mainly transsynaptically. Brain Stimul. *8*, 742–750.
22. Kumaravelu, K., Sombeck, J., Miller, L.E., Bensmaia, S.J., and Grill, W.M. (2022). Stoney vs. histed: quantifying the spatial effects of intracortical microstimulation. Brain Stimul. *15*, 141–151.
23. Houweling, A.R., and Brecht, M. (2008). Behavioural report of single neuron stimulation in somatosensory cortex. Nature *451*, 65–68.
24. Butovas, S., and Schwarz, C. (2003). Spatiotemporal effects of microstimulation in rat neocortex: a parametric study using multielectrode recordings. J. Neurophysiol. *90*, 3024–3039.
25. Hao, Yaoyao, Riehle, A., and Brochier, T.G. (2016). Mapping horizontal spread of activity in monkey motor cortex using single pulse microstimulation. Front. Neural Circuits *10*, 104.
26. Butovas, S., Hormuzdi, S.G., Monyer, H., and Schwarz, C. (2006). Effects of electrically coupled inhibitory networks on local neuronal responses to intracortical microstimulation. J. Neurophysiol. *96*, 1227–1236.
27. Venkatraman, S., and Carmena, J.M. (2009). Behavioral modulation of stimulus-evoked oscillations in barrel cortex of alert rats. Front. Integr. Neurosci. *3*, 10.
28. Ruff, D.A., and Cohen, M.R. (2016). Attention increases spike count correlations between visual cortical areas. J. Neurosci. *36*, 7523–7534.
29. Cicmil, Nela, Cumming, B.G., Parker, A.J., and Krug, K. (2015). Reward modulates the effect of visual cortical microstimulation on perceptual decisions. eLife *4*, e07832.
30. Butovas, S., and Schwarz, C. (2022). Local neuronal responses to intracortical microstimulation in rats' barrel cortex are dependent on behavioral context. Front. Behav. Neurosci. *16*, 805178.
31. Bradley, C., Nydam, A.S., Dux, P.E., and Mattingley, J.B. (2022). State-dependent effects of neural stimulation on brain function and cognition. Nat. Rev. Neurosci. *23*, 01234567.
32. Brugger, D., Butovas, S., Bogdan, M., and Schwarz, C. (2011). Real-time adaptive microstimulation increases reliability of electrically evoked cortical potentials. IEEE Trans. Biomed. Eng. *58*, 1483–1491.
33. Yun, R., Mishler, J.H., Perlmutter, S.I., Rao, R.P.N., and Fetz, E.E. (2023). Responses of cortical neurons to intracortical microstimulation in awake primates. eNeuro. *10*, 0336–22.2023.
34. Geva-Sagiv, M., Mankin, E.A., Eliashiv, D., Epstein, S., Cherry, N., Kalender, G., Tchemodanov, N., Nir, Y., and Fried, I. (2023). Augmenting hippocampal-prefrontal neuronal synchrony in human sleep enhances memory consolidation. Nat. Neurosci. *26*, 1100–1110.
35. Histed, M.H., Bonin, V., and Reid, R.C. (2009). Direct activation of sparse, distributed populations of cortical neurons by electrical microstimulation. Neuron *63*, 508–522.
36. Voigt, M.B., Yusuf, P.A., and Kral, A. (2018). Intracortical microstimulation modulates cortical induced responses. J. Neurosci. *38*, 7774–7786.
37. Sombeck, J.T., Heye, J., Kumaravelu, K., Goetz, S.M., Peterchev, A.V., Grill, W.M., Bensmaia, S., and Miller, L.E. (2022). Characterizing the short-latency evoked response to intracortical microstimulation across a multi-electrode array. J. Neural Eng. *19*, 026044.
38. Dadarlat, M.C., Sun, Y., and Stryker, M.P. (2019). Widespread activation of awake mouse cortex by electrical stimulation. Int. IEEE EMBS Conf. Neural Eng. 2019, 1113–1117.
39. Xie, Y., Heida, T., Stegenga, J., Zhao, Y., Moser, A., Tronnier, V., Feuerstein, T.J., and Hofmann, U.G. (2014). High-frequency electrical stimulation

suppresses cholinergic accumbens interneurons in acute rat brain slices through GABAB receptors. Eur. J. Neurosci. *40*, 3653–3662.

40. Haider, B., Häusser, M., and Carandini, M. (2013). Inhibition dominates sensory responses in the awake cortex. Nature *493*, 97–100.
41. Sellers, K.K., Bennett, D.V., Hutt, A., Williams, J.H., and Fröhlich, F. (2015). Awake vs. anesthetized: layer-specific sensory processing in visual cortex and functional connectivity between cortical areas. J. Neurophysiol. *113*, 3798–3815.
42. Michelson, N.J., and Kozai, T.D.Y. (2018). Isoflurane and ketamine differentially influence spontaneous and evoked laminar electrophysiology in mouse V1. J. Neurophysiol. *120*, 2232–2245.
43. McIntyre, C.C., Grill, W.M., Sherman, D.L., and Thakor, N.V. (2004). Cellular effects of deep brain stimulation: model-based analysis of activation and inhibition. J. Neurophysiol. *91*, 1457–1469.
44. Taniguchi, H., He, M., Wu, P., Kim, Sangyong, Paik, R., Sugino, K., Kvitsiani, D., Fu, Y., Lu, J., Lin, Y., et al. (2011). A resource of cre driver lines for genetic targeting of GABAergic neurons in cerebral cortex. Neuron *71*, 995–1013.
45. Ledri, M., Madsen, M.G., Nikitidou, L., Kirik, D., and Kokaia, M. (2014). Global optogenetic activation of inhibitory interneurons during epileptiform activity. J. Neurosci. *34*, 3364–3377.
46. Lee, S., Hjerling-Leffler, J., Zagha, E., Fishell, G., and Rudy, B. (2010). The largest group of superficial neocortical GABAergic interneurons expresses ionotropic serotonin receptors. J. Neurosci. *30*, 16796–16808.
47. Chen, T.W., Wardill, T.J., Sun, Y., Pulver, S.R., Renninger, S.L., Baohan, A., Schreiter, E.R., Kerr, R.A., Orger, M.B., Jayaraman, V., et al. (2013). Ultrasensitive fluorescent proteins for imaging neuronal activity. Nature *499*, 295–300.
48. Stoney, S.D., Thompson, W.D., and Asanuma, H. (1968). Excitation of pyramidal tract cells by intracortical microstimulation: effective extent of stimulating current. J. Neurophysiol. *31*, 659–669.
49. Komarov, M., Malerba, P., Golden, R., Nunez, P., Halgren, E., and Bazhenov, M. (2019). Selective recruitment of cortical neurons by electrical stimulation. PLOS Comput. Biol. *15*, e1007277.
50. Eles, J.R., and Kozai, T.D.Y. (2020). vivo imaging of calcium and glutamate responses to intracortical microstimulation reveals distinct temporal responses of the neuropil and somatic compartments in layer II/III neurons. Biomaterials *234*, 119767.
51. Niell, C.M., and Stryker, M.P. (2010). Modulation of visual responses by behavioral state in mouse visual cortex. Neuron *65*, 472–479.
52. McGinley, M.J., Vinck, M., Reimer, J., Batista-Brito, R., Zagha, E., Cadwell, C.R., Tolias, A.S., Cardin, J.A., and McCormick, D.A. (2015). Waking state: rapid variations modulate neural and behavioral responses. Neuron *87*, 1143–1161.
53. Vinck, M., Batista-Brito, R., Knoblich, U., and Cardin, J.A. (2015). Arousal and locomotion make distinct contributions to cortical activity patterns and visual encoding. Neuron *86*, 740–754.
54. Recanzone, G.H., Merzenich, M.M., and Dinse, H.R. (1992). Expansion of the cortical representation of a specific skin field in primary somatosensory cortex by intracortical microstimulation. Cereb. Cortex *2*, 181–196.
55. Dinse, H.R., Recanzone, G.H., and Merzenich, M.M. (1993). Alterations in correlated activity parallel ICMS- induced representational plasticity. NeuroReport *5*, 173–176.
56. Callaway, E.M. (2016). Inhibitory cell types, circuits and receptive fields in mouse visual cortex. In Micro-, Meso- and Macro-Connectomics of the Brain, H. Kennedy, et al., eds., pp. 11–18.
57. Pfeffer, C.K., Xue, M., He, M., Huang, Z.J., and Scanziani, M. (2013). Inhibition of inhibition in visual cortex: the logic of connections between molecularly distinct interneurons. Nat. Neurosci. *16*, 1068–1076.
58. Hofer, S.B., Ko, H., Pichler, B., Vogelstein, J., Ros, H., Zeng, H., Lein, E., Lesica, N.A., and Mrsic-Flogel, T.D. (2011). Differential connectivity and response dynamics of excitatory and inhibitory neurons in visual cortex. Nat. Neurosci. *14*, 1045–1052.
59. Lee, S.H., Kwan, A.C., Zhang, S., Phoumthipphavong, V., Flannery, J.G., Masmanidis, S.C., Taniguchi, H., Huang, Z.J., Zhang, F., Boyden, E.S., et al. (2012). Activation of specific interneurons improves V1 feature selectivity and visual perception. Nature *488*, 379–383.
60. Rikhye, R.V., Yildirim, M., Hu, M., Breton-Provencher, V., and Sur, M. (2021). Reliable sensory processing in mouse visual cortex through cooperative interactions between somatostatin and parvalbumin interneurons. J. Neurosci. *41*, 8761–8778.
61. Agetsuma, M., Hamm, J.P., Tao, K., Fujisawa, S., and Yuste, R. (2018). Parvalbumin-positive interneurons regulate neuronal ensembles in visual cortex. Cereb. Cortex *28*, 1831–1845.
62. Fu, Y., Tucciarone, J.M., Espinosa, J.S., Sheng, Nengyin, Darcy, D.P., Nicoll, R.A., Huang, Z.J., and Stryker, M.P. (2014). A cortical circuit for gain control by behavioral state. Cell *156*, 1139–1152.
63. Overstreet, C.K., Klein, J.D., and Helms Tillery, S.I. (2013). Computational modeling of direct neuronal recruitment during intracortical microstimulation in somatosensory cortex. J. Neural Eng. *10*, 066016.
64. Beaulieu, C. (1993). Numerical data on neocortical neurons in adult rat, with special reference to the GABA population. Brain Res. *609*, 284–292.
65. Lefort, S., Tomm, C., Floyd Sarria, J.C.F., and Petersen, C.C.H. (2009). The excitatory neuronal network of the C2 barrel column in mouse primary somatosensory cortex. Neuron *61*, 301–316.
66. Griffin, D.M., Hudson, H.M., Belhaj-Saïf, A., and Cheney, P.D. (2011). Hijacking cortical motor output with repetitive microstimulation. J. Neurosci. *31*, 13088–13096.
67. Cheney, P.D., Griffin, D.M., and Van Acker, G.M. (2013). Neural hijacking: action of high-frequency electrical stimulation on cortical circuits. Neuroscientist *19*, 434–441.
68. Murris, S.R., Arsenault, J.T., and Vanduffel, W. (2020). Frequency- and state-dependent network effects of electrical stimulation targeting the ventral tegmental area in macaques. Cereb. Cortex *30*, 4281–4296.
69. Scangos, K.W., Makhoul, G.S., Sugrue, L.P., Chang, E.F., and Krystal, A.D. (2021). State-dependent responses to intracranial brain stimulation in a patient with depression. Nat. Med. *27*, 229–231.
70. Yang, Y., Qiao, S., Sani, O.G., Sedillo, J.I., Ferrentino, B., Pesaran, B., and Shanechi, M.M. (2021). Modelling and prediction of the dynamic responses of large-scale brain networks during direct electrical stimulation. Nat. Biomed. Eng. *5*, 324–345.
71. Kara, P., Pezaris, J.S., Yurgenson, S., and Reid, R.C. (2002). The spatial receptive field of thalamic inputs to single cortical simple cells revealed by the interaction of visual and electrical stimulation. Proc. Natl. Acad. Sci. USA *99*, 16261–16266.
72. Weihberger, O., Okujeni, S., Mikkonen, J.E., and Egert, U. (2013). Quantitative examination of stimulus-response relations in cortical networks in vitro. J. Neurophysiol. *109*, 1764–1774.
73. de Castro, M.C., and Cliquet, A. (2000). Artificial sensorimotor integration in spinal cord injured subjects through neuromuscular and electrotactile stimulation. Artif. Organs *24*, 710–717.
74. Raspopovic, S., Capogrosso, M., Petrini, F.M., Bonizzato, M., Rigosa, J., Di Pino, G., Carpaneto, J., Controzzi, M., Boretius, T., Fernandez, E., et al. (2014). Restoring natural sensory feedback in real-time bidirectional hand prostheses. Sci. Transl. Med. *6*, 222ra19.
75. Tabot, G.A., Kim, S.S., Winberry, J.E., and Bensmaia, S.J. (2015). Restoring tactile and proprioceptive sensation through a brain interface. Neurobiol. Dis. *83*, 191–198.
76. Dadarlat, M.C., O'Doherty, J.E., and Sabes, P.N. (2015). A learning-based approach to artificial sensory feedback leads to optimal integration. Nat. Neurosci. *18*, 138–144.
77. Richardson, A.G., Ghenbot, Y., Liu, X., Hao, H., Rinehart, C., DeLuccia, S., Torres Maldonado, S., Boyek, G., Zhang, M., Aflatouni, F., et al. (2019). Learning active sensing strategies using a sensory brain–machine interface. Proc. Natl. Acad. Sci. USA *116*, 116.35.

78. Ni, A.M., and Maunsell, J.H.R. (2010). Microstimulation reveals limits in detecting different signals from a local cortical region. Curr. Biol. *20*, 824–828.

79. Pancholi, R., Ryan, L., and Peron, S. (2023). Learning in a sensory cortical microstimulation task is associated with elevated representational stability. Nat. Commun. *14*, 3860.

80. Akitake, B., Douglas, H.M., LaFosse, P.K., Beiran, M., Deveau, C.E., O'Rawe, J., Li, A.J., Ryan, L.N., Duffy, S.P., Zhou, Z., et al. (2023). Amplified cortical neural responses as animals learn to use novel activity patterns. Curr. Biol. *33*, 2163–2174.e4.

81. Madisen, L., Zwingman, T.A., Sunkin, S.M., Oh, S.W., Zariwala, H.A., Gu, H., Ng, L.L., Palmiter, R.D., Hawrylycz, M.J., Jones, A.R., et al. (2010). A robust and high-throughput Cre reporting and characterization system for the whole mouse brain. Nat. Neurosci. *13*, 133–140.

82. Niell, C.M., and Stryker, M.P. (2008). Highly selective receptive fields in mouse visual cortex. J. Neurosci. *28*, 7520–7536.

83. Dadarlat, M.C., and Stryker, M.P. (2017). Locomotion enhances neural encoding of visual stimuli in mouse V1. J. Neurosci. *37*, 3764–3775.

84. Goldey, G.J., Roumis, D.K., Glickfeld, L.L., Kerlin, A.M., Reid, R.C., Bonin, V., Schafer, D.P., and Andermann, M.L. (2014). Removable cranial windows for long-term imaging in awake mice. Nat. Protoc. *9*, 2515–2538.

85. Dombeck, D.A., Khabbaz, A.N., Collman, F., Adelman, T.L., and Tank, D.W. (2007). Imaging large-scale neural activity with cellular resolution in awake, mobile mice. Neuron *56*, 43–57.

86. Rousche, P.J., and Normann, R.A. (1999). Chronic intracortical microstimulation (ICMS) of cat sensory cortex using the utah intracortical electrode array. IEEE Trans. Rehabil. Eng. *7*, 56–68.

87. McCreery, D.B., Agnew, W.F., Yuen, T.G.H., and Bullara, L. (1990). Charge density and charge per phase as cofactors in neural injury induced by electrical stimulation. IEEE Trans. Bio Med. Eng. *37*, 996–1001.

88. McCreery, D.B., Yuen, T.G.H., Agnew, W.F., and Bullara, L.A. (1994). Stimulus parameters affecting tissue injury during microstimulation in the cochlear nucleus of the cat. Hear. Res. *77*, 105–115.

89. Pachitariu, M., Stringer, C., Dipoppa, M., Schröder, S., Rossi, L.F., et al. (2016). Suite2p: beyond 10,000 neurons with standard two-photon microscopy. bioRxiv, 061507.

90. Stringer, C., Pachitariu, M., Steinmetz, N., Carandini, M., and Harris, K.D. (2019). High-dimensional geometry of population responses in visual cortex. Nature *571*, 361–365.

STAR★METHODS

KEY RESOURCES TABLE

REAGENT or RESOURCE	SOURCE	IDENTIFIER
Bacterial and virus strains		
AAV1.Syn.GCaMP6s.WPRE.SV40	Addgene	RRID:Addgene_100843
Deposited data		
Data and custom analysis code	This manuscript	Mendely Data: https://doi.org/10.17632/tzwps2dykh.1
Experimental models: Organisms/strains		
Gad2-IRES-Cre	Jackson Laboratory	RRID:IMSR_JAX:010802
Ai14	Jackson Laboratory	RRID:IMSR_JAX:007914
Software and algorithms		
MATLAB	Mathworks	mathworks.com
Suite2P	Pachitariu Lab	https://github.com/MouseLand/suite2p
Other		
platinum/iridium (Pt/Ir) electrode	Microprobes	Cat#PI20030.1A3

RESOURCE AVAILABILITY

Lead contact

Further information and requests for resources should be directed to and will be fulfilled by the lead contact, Maria C. Dadarlat (mdadarla@purdue.edu).

Materials availability

This study did not generate new unique reagents.

Data and code availability

The data and custom analysis code is available at Mendeley Data: https://doi.org/10.17632/tzwps2dykh.1. Any questions regarding the analysis should be directed to the lead contact, Maria C. Dadarlat.

METHOD DETAILS

Surgery

All procedures were conducted in accordance with the ethical guidelines of the National Institutes of Health and were approved by the Institutional Animal Care and Use Committee at the University of California, San Francisco. The surgical procedures used in these experiments have been described previously[38] and are related briefly below. The overall experimental setup is shown in Figure 1.

Mouse cortical inhibitory neurons were labeled with red fluorescent markers by crossing transgenic mouse lines Gad2-IRES-Cre with reporter line Ai14 (Jackson labs strains 010802 and 007914;[44,81]). We studied five mice of ages 3–6 months (both male and female). Each mouse underwent a total of three separate surgical procedures to chronically implant 1) a titanium headplate, 2) a platinum/iridium (Pt/Ir) electrode (0.1 MOhm, PI20030.1A3 Microprobes for Life Sciences) beneath a glass cranial window, and 3) a two-pin receptacle connector and ground wire. Just prior to implantation of the stimulating electrode, mice were injected with 100 nL of AAV virus expressing GCaMP6s into three locations within primary visual cortex (AAV1.Syn.GCaMP6s.WPRE.SV40) at two depths (150 and 300 μ m) per location. AAV1.Syn.GCaMP6s.WPRE.SV40 was a gift from Douglas Kim & GENIE Project (Addgene viral prep # 100843-AAV1; http://n2t.net/addgene:100843; RRID:Addgene_100843). This virus transfects both excitatory and inhibitory neurons with a fast fluorescent indicator of calcium concentration. For each procedure, animals were anesthetized to areflexia using a mixture of Ketamine and Xylazine (100 mg/kg and 5 mg/kg, IP).

The surgery to implant a titanium headplate was previously described in detail.[82,83] The headplates used here were modified from the original design by removing the rear third, leaving a semicircular portion with lateral flanges. We implanted the Pt/Ir stimulating electrode and glass cranial window between three to seven days after the headplate surgery. Implantation of the glass cranial window closely follows well-established experimental protocols.[84,85] The stimulating electrode was implanted after a craniotomy was made to expose the cortical surface. Following drilling of the skull but prior to removal of the bone flap, a small ramp was shaved in the skull just anterior

to the craniotomy. This ramp allowed us to implant the stimulating electrode at the very edge of the craniotomy – a detail that was critical for successfully securing the glass cranial window onto the surface of the brain and ensuring a long-lasting chronic implant.

The Pt/Ir electrode was inserted at a 7 or 11 degree angle to a targeted depth of 150–200 μ m below the cortical surface using a digital micromanipulator (Sutter MP-285). However, using 2-photon imaging to estimate electrode depth prior to completing recordings, we found that the actual implantation depth varied from 100 - 150. Next, a layer of sterile Vaseline was placed along the posterior of the craniotomy behind which a layer of cyanoacrylate mixed with dental acrylic was added to fix the electrode in place. After the electrode was secure and the Vaseline removed, a 3 mm glass window was placed over the craniotomy. The edges of the window were fixed in place using cyanoacrylate, and were further stabilized by the application of dental acrylic. The electrode was clipped with wire cutters at its exit from the dental cement, leaving only an edge exposed.

After allowing the animal to recover for several days, a two-pin receptacle connector and ground wire were implanted. One pin of the connector was electrically connected to the end of the implanted electrode using a conductive silver paint. The connection was insulated using cyanoacrylate, and the rest of the connector was firmly attached to the rear of the titanium headplate using more cyanoacrylate. To complete the circuit, a small hole was drilled through the skull over the contralateral frontal lobe. The stripped end of a chloridized silver wire was inserted beneath the skull (making contact with cerebral spinal fluid but not piercing the brain) and the opening was covered with a biocompatible silicone elastomer. Finally, cyanoacrylate was applied over the silicone elastomer and over any loose portion of the ground wire to provide stability and electrical insulation. The headplate, electrode, and glass imaging window were thus chronically implanted for the duration of the experiments. This surgery typically provided stable images for three to six months following implantation. However, the experiments reported here took place on a single day during a single recording and stimulation session.

Electrical stimulation

The goal of the experimental protocol was to understand how electrical stimulation of a range of amplitudes modulates activity in surrounding neurons and to isolate differences in its effect on excitatory and inhibitory neurons. The stimulation protocol consisted of delivering a constant-current electrical stimulus of nine different intensities once every ten seconds, for a total of ninety stimuli during the recording session (Figure 1C). The amplitude of each stimulus was chosen from an array of possible values (3, 5, 10, 15, 20, 25, 30, 40, or 50 μA) in a pseudo-random fashion, for a total of ten repetitions per stimulus amplitude across the experimental session. Stimulation frequency was held fixed at 250 Hz. Each stimulus consisted of a train of twenty-five biphasic, cathode-leading pulses for a total stimulation duration of 100 ms. Biphasic pulses were composed of a 200 μs cathodal pulse, a 200 μs inter-pulse interval, and a 200 μs anodal pulse. Based on analysis of current density as a function of surface area of the stimulating electrode, we do not expect stimulation at these levels to have damaged cortical tissue. The exposed tip of the chronically-implanted stimulating electrode is approximately 3900 μm^2 (personal communication with Microprobes for Life Sciences). In contrast, the exposed tip of the Utah array is estimated to be 1573 μm^2.[86] We used a maximum stimulation amplitude of 50 μ A at 200 μs duration for a total pulse delivery of 10 nC per phase or 0.01 μ C per phase. Taking into account the area of the exposed tip, this translates into 5.8 μ C/(ph cm^2), which is expected to do no damage to the surrounding neural tissue in the context of this experiment.[87] However, note that prolonged stimulation at stimulation amplitudes above 3 nC per phase is known to cause damage to the cortex.[88]

Two-photon calcium imaging

Calcium responses of specific cell types and processes were acquired using a resonant-scanning two photon microscope (Neurolabware) controlled by Scanbox acquisition software. A Coherent Chameleon Ultra II laser was used for GCaMP excitation at a wavelength of 920 nm. Emission light was filtered by emission filters (525/70 and 610/75 nm) and measured by two independent photomultiplier tubes (Hamamatsu R3896). The objective used was a 16x water-immersion lens (Nikon, 0.8 numerical aperture (NA), 3 mm working distance). Image sequences were captured at 15.5 Hz at a depth of 100–300 μ m below the pia. All recordings were made on awake, head-fixed mice that were free to walk or run on a spherical ball that is elevated by a stream of air[85] (Figure 1B).

Neural responses were imaged in three planes spaced 20 μm apart in depth, covering an area of approximately one μm^2 (1136 μm by 1083 μm). Each plane was imaged at 5.17 Hz (15.5 Hz divided by three imaging planes). In four of the mice, the first imaging plane was at placed the depth of the stimulating electrode (assessed by visual inspection or automated z-stack imaging) and the remaining two planes were 20 and 40 μm deeper. In one mouse, imaging depth was restricted (possibly by viral expression levels), so we instead placed imaging planes at the electrode tip and 20 μm above and below the electrode tip. All neural recordings were made in a dark room and the animals were isolated from the experimenter in an enclosure formed by black laser safety fabric. Mice underwent at least 5 days of training to acclimate to the treadmill and head-fixation prior to recordings. Treadmill movement was captured by a Dalsa Genie M1280 camera synchronized to microscope scanning.

QUANTIFICATION AND STATISTICAL ANALYSIS

Registration, cell detection, and neuropil correction

Image registration, region of interest (ROI) detection, neuropil correction of the two-photon imaging data were carried out using the Suite2p pipeline.[89] The data were further curated through manual cell detection, differentiating between cell and non-cell ROIs using

the Suite2p GUI. Each ROI identified by Suite2p was manually analyzed to determine whether Suite2p's classification of cell or non-cell was correct. The classifier was trained by considering the calcium traces, shape, compactness, aspect ratio and position of the ROIs. ROIs were considered as cells if: 1) they had calcium traces considerably different from the surrounding neuropil activity, and 2) a round, compact shape of a size large enough to represent a cell body rather than the cross section of a dendrite. We kept all ROIs that were assigned by Suite2p a probability of at least 0.5 of being a neuron. All subsequent analyses were conducted in Matlab using custom code.

Electrical stimulation induced a large, synchronized deviation of the neuropil signal, which may bias the responses recorded in "single-neuron" ROIs. Therefore, to isolate a single neuron's activity across the imaging session, we subtracted 0.8 times the neuropil signal surrounding each cell (neuropil was assumed to be an annulus surrounding each ROI). Note that this value is larger than that conventionally used[90] to account for the high level of neuropil synchrony during electrical stimulation. We arrived at a value of 0.8 for neuropil subtraction following qualitative inspection of non-neuronal regions of interest, ensuring that response traces neither had residual neuropil contamination nor were artificially suppressed following neuropil subtraction.

Identification of inhibitory neurons

Red cells (genetically labeled inhibitory neurons) were determined by detecting ROIs from the red channel, based on modification from suite2p source code. Briefly, pixels on averaged images from the green and red channels were plotted as x vs. y (green vs. red) to generate a linear fit to estimate the potential contribution in the red channel from the green channel: instead of using least square method, we used the minimum value of the red channel against values of each green channel. After subtraction of the estimated contribution from green channel, the red signal in each ROI was then calculated and compared with nearby ROIs: if it was significantly greater than the local average (2 times of the standard deviation), the cell was classified as inhibitory neurons.

Radial distance from electrode tip

To describe stimulation-evoked activity patterns as a function of radial distance from the electrode tip, each neuron's relative position was calculated as follows. The position of the electrode tip was found by visually inspecting the max projection image across the aligned imaging movie data. Within each imaging plane, a neuron's position was said to be at the mean of the x and y pixels assigned to that ROI, which were then converted into μ m. We found the radial distance for each neuron, r, by including information about the imaging plane in which each ROI was located: $r = (x^2+y^2+z^2)^{\frac{1}{2}}$, where x and y are the mean position of a neuron within the imaging plane (in mm) and z is the distance between the plane of the electrode tip and that of the ROI (0, 20, or 40 μ m). Once the relative position of each cell was found, we binned all distances into bins of width 100 μ m, ranging from 0 to 500 μ m.

3D Volume from electrode tip

The cortical volume associated with stimulation-evoked activity is defined as the three-dimensional space taken up by activated neurons if a boundary were to be drawn around the outermost neurons. We use this metric instead of the more conventional calculation of radial distance of a sphere[17] because the boundary calculation allows for anisotropic current flow (and thus activation patterns) during stimulation.

Significant modulation of neural activity

Neural responses to stimulation were characterized as the change in fluorescent intensity of the cell body for 20 samples relative to its value at stimulation onset. This data spanned 3.67 seconds at 5.17 Hz sampling rate per imaging plane, with the first time point taken to be the sample just prior to when stimulation occurred. A neural "response" was said to be the fluorescent activity within the region of interest defined for each neuron in the four seconds, starting at and including the point of stimulation. The responses of calcium florescence were split into 2 stages: stage 1 (approximately 0-580 ms, which is equivalent to taking 3 data samples including the time-point of stimulation) and stage 2 (580 - 3680 ms after stimulation — the subsequent 16 samples). This criteria was based on the approximately time it took for a GCaMP6s florescent signal that corresponded to ten action potentials to rise and plateau (up to 500 - 600 ms for ten spikes, although rise time was lower for fewer spikes;[47]).

To determine significant modulation by electrical stimulation, we compared early and late stage responses for the ten trials at each amplitude with the neuron's single-trial baseline activity (calculated as the average activity in the three second period prior to stimulation onset). Significant deviation from baseline (taken as the 3 s preceding stimulation onset) was tested for the early and late stage separately using a Wilcoxon rank-sum test, taking $p \leq 0.02$ as a threshold. No corrections were made for multiple comparisons; instead, further analysis takes this level of activation (one out of every 50 neurons considered) to be equal to chance.

Removal of data following high-amplitude trials

One limitation of measuring neural activity using calcium imaging is the slow decay rates contributed by both the nature of the calcium influx and genetically-encoded calcium indicators. To mitigate the possibility that neural suppression was an artifact of slow GCaMP6s decay following high-amplitude stimulation, we only analyzed neural responses for significance after removing any data that followed high-amplitude trials. High-amplitude stimulation was defined as those in which the duration of fluorescence decay had not returned to baseline by the beginning of the next stimulus trials (Figure 3A). This was found to occur for 30, 40, and 50 μ A for short-latency excitation. Our results did not greatly change when we additionally designated 25 μ A as high-amplitude; however, the

number of trials that could be considered to determine modulation significance fell, so we chose to present the results when keeping trials following 25 μ A stimulation.

Amplitude and variance of evoked neural responses

The amplitude of an evoked neural response was calculated in one of two ways. The first method, used in Figure 2, simply took the maximum value of a neuron's average response (a four second trace of fluorescence as a function of time, beginning at the time of stimulation) to each stimulation amplitude (averaged across ten trials). To account for neurons that were predominantly suppressed by stimulation, we also found the minimum of the trial-averaged response trace. Then, the modulation amplitude for that neuron was taken as the maximum of two values: the absolute value of the minimum and the maximum of the response. The second method, used in Figure 3, takes into account the temporal response of each neuron (see below description of neural response profiles) when calculating response amplitude. In this case, the response amplitude was taken to be the average value of the response stage in which the neuron was significantly modulated. This analysis splits apart suppression from excitation. If the neuron was significantly modulated during both stages, we took the response amplitude to be the maximum of the absolute value of the average activity evoked in each stage (to account for negative Δ F values during suppression).

Establishing neural response profiles

Based on prior literature, we know that neurons can be excited, suppressed, or both by electrical stimulation at varying time lags relative to stimulation onset. To categorize the temporal responses of neurons and to catalog their diversity, we considered eight possible combination of significant response patterns:

1 Significant excitation only in stage 1
2 Significant excitation in both stages
3 Significant excitation only in stage 2
4 Significant excitation in stage 1 followed by significant suppression in stage 2
5 Significant suppression only in stage 1
6 Significant suppression in both stages
7 Significant suppression only in stage 2
8 Significant suppression in stage 1 followed by significant excitation in stage 2

Of these eight categories, the majority of responses fell into groups 1, 2, 3, and 7. Therefore, we simplified our characterization of neural responses into into four major categories: short-latency excitation (response profiles 1, 2), long-latency excitation (response profiles 3), short-latency suppression (response profiles 5, 6, 8), and long-latency suppression (response profiles 4 and 7).

Neural correlations and Effect size

To determine the effect of ongoing neural activity levels and overt motor behavior on stimulation-evoked neural responses, we first calculated pairwise correlations for single neurons between a neuron's mean evoked response to stimulation and: 1) baseline neural activity level prior to stimulation, 2) stimulation amplitude, and 3) running speed. We additionally shuffled the trial order as a control to generate distributions for random correlations. The correlation was computed for each cell across all trials, excluding trials that followed high-amplitude stimulation trials (30, 40, or 50 μ A).

Next, for each neuron, we calculated an ''effect size'' for the effect of differences in pre-stimulus neural activity on the amplitude of stimulation-evoked responses. The pre-stimulus neural activity was taken to be the average fluorescence of the neuron in the 1 s preceding stimulation. The effect size was set to the slope of the linear regression parameters fit to model the mean evoked response (y) as a function of pre-stimulus neural activity (x). The effect size was calculated separately for each stimulation amplitude after excluding trials that followed high-amplitude stimulation (30, 40, or 50 μ A).

The amount of variance in the response amplitude that is accounted for by pre-stimulus activity is equal to the R^2 value of the linear regression. We first calculated an effect size for each neuron at each stimulation amplitude (assigning a NaN value if the neuron was not significantly modulated by stimulation at a particular amplitude). Then, to measure the relationship between current amplitude, radial distance from the electrode tip, and variance explained, we first took all the neurons that were significantly modulated at each stimulation amplitude and then binned them into groups as a function of distance. Finally, we calculated the the average R^2 across those neurons at each combination of distance and stimulation amplitude.

Neuron, Volume *112*

Supplemental information

Activity-dependent recruitment of inhibition and excitation in the awake mammalian cortex during electrical stimulation

Maria C. Dadarlat, Yujiao Jennifer Sun, and Michael P. Stryker

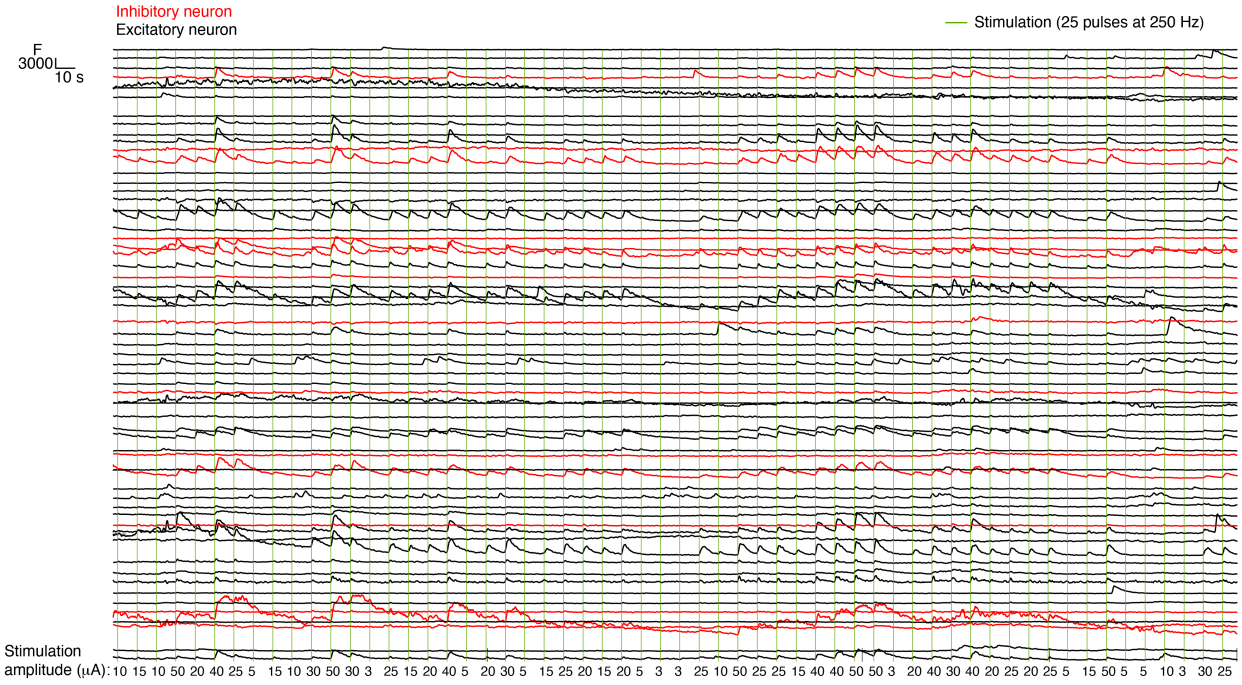

Supplemental Figure 1: Sample single-neuron responses from inibitory (red) and excitatory (black) neurons during stimulation trials, related to Figure 1. Traces show changes in the fluorescent signal within regions of interest and have been corrected for neuropil contamination.

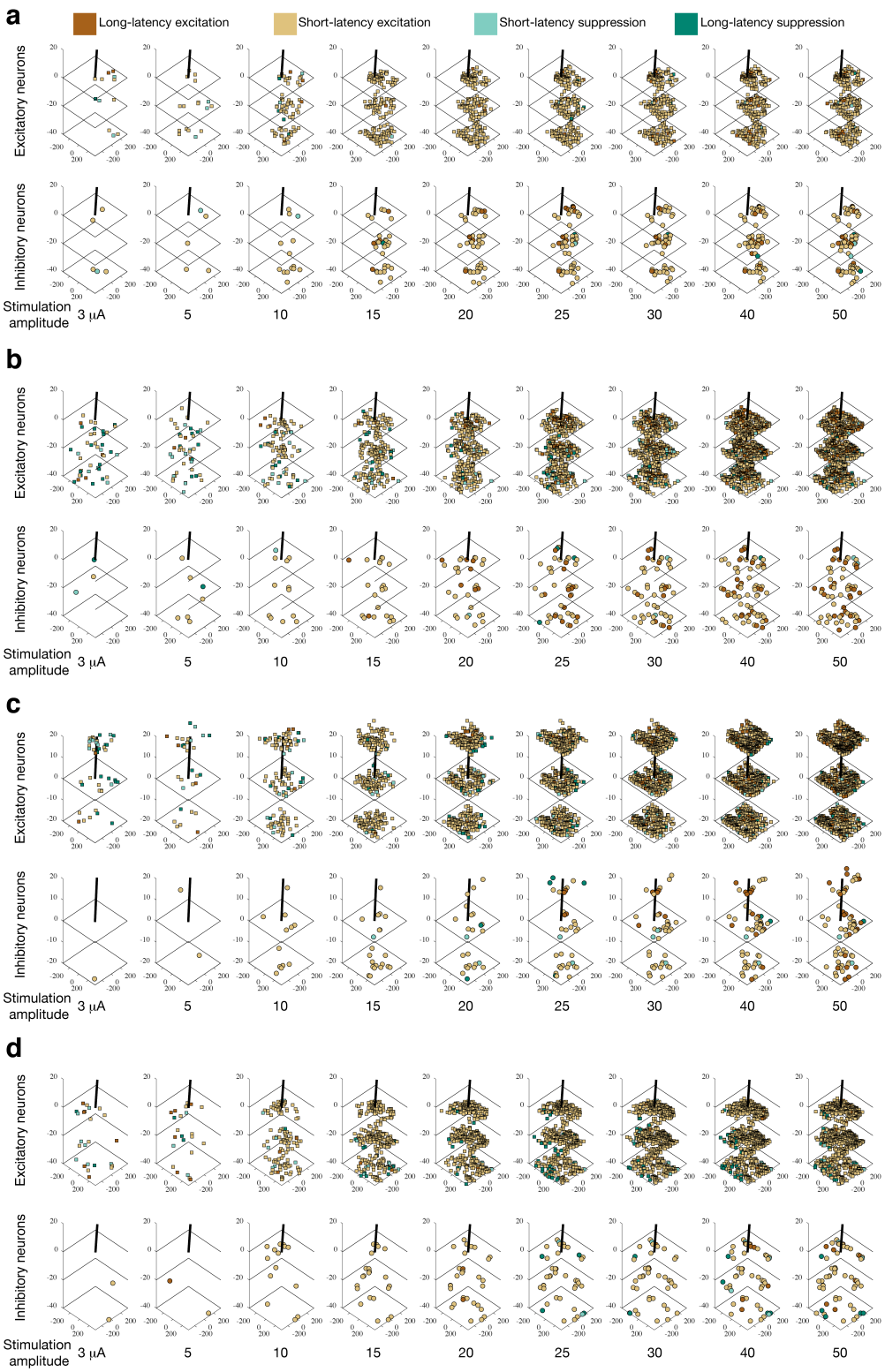

Supplemental Figure 2: Spatial distribution of stimulation-evoked responses as a function of stimulation amplitude for excitatory neurons (top row) and inhibitory neurons (bottom row) for each of four experimental mice (not including mouse from main text), related to Figure 4. Black line designates the electrode. Three stacked imaging planes are shown, each 20 *mu*m apart. Colors indicate response type (long-latency excitation, short-latency excitation, short-latency inhibition, long-latency inhibition). Axis label are in mm.

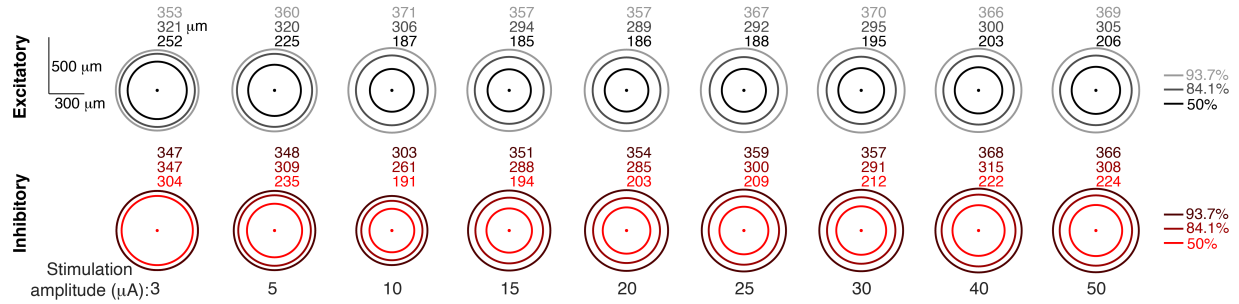

Supplemental Figure 3: The radial distribution of neurons activated by electrical stimulation is depicted by the radial width of a set of concentric circles, shown at 50, 84.1, and 93.7 percentiles of the distribution for each stimulation amplitude, related to Figure 4. The numerical value of the radial distance at each percentile is shown above each group of circles.